Available online at www.sciencedirect.com
ScienceDirect
Journal of Sound and Vibration 317 (2008) 329–353
JOURNAL OF SOUND AND VIBRATION
www.elsevier.com/locate/jsvi

Three-dimensional free vibration analysis of isotropic rectangular plates using the B-spline Ritz method

H. Nagino[a,*], T. Mikami[a], T. Mizusawa[b]

[a]*Division of Engineering and Policy for Cold Regional Environment, Graduate School of Engineering, Hokkaido University, Kita 13 Nishi 8, Kita-ku, Sapporo 060-8628, Japan*
[b]*Department of Civil Engineering and Environment Design, Daido Institute of Technology, Hakusui-cho 40, Minami-ku, Nagoya 457-0818, Japan*

Received 10 October 2006; received in revised form 14 March 2008; accepted 16 March 2008
Handling Editor: L.G. Tham
Available online 12 May 2008

Abstract

This paper presents three-dimensional free vibration analysis of isotropic rectangular plates with any thicknesses and arbitrary boundary conditions using the B-spline Ritz method based on the theory of elasticity. The proposed method is formulated by the Ritz procedure with a triplicate series of B-spline functions as amplitude displacement components. The geometric boundary conditions are numerically satisfied by the method of artificial spring. To demonstrate the convergence and accuracy of the present method, several examples with various boundary conditions are solved, and the results are compared with other published solutions by exact and other numerical methods based on the theory of elasticity and various plate theories. Rapid, stable convergences as well as high accuracy are obtained by the present method. The effects of geometric parameters on the vibrational behavior of cantilevered rectangular plates are also investigated. The results reported here may serve as benchmark data for finite element solutions and future developments in numerical methods.

1. Introduction

Isotropic rectangular plates are commonly used as structural components in aerospace, nuclear, marine, electronic, and structural engineering applications. These plates are often subjected to complicated external dynamic loads such as earthquakes, impacts, movable loadings and other conditions. Therefore, an understanding of the free vibrational behavior for low- and high-order frequencies is very important in structural design. Three-dimensional (3-D) free vibration analysis is based on the theory of elasticity and does not rely on hypotheses involving the kinematics of deformation. Therefore, 3-D free vibration analysis provides realistic results as well as it also provides physical insights which cannot otherwise be predicted by shear deformation plate theories [1–7].

*Corresponding author. Tel.: +81 11 706 6176; fax: +81 11 706 6174.
E-mail address: nagino@oita-ct.ac.jp (H. Nagino).

0022-460X/$ - see front matter © 2008 Elsevier Ltd. All rights reserved.
doi:10.1016/j.jsv.2008.03.021

Despite the practical importance of 3-D free vibration of isotropic thick rectangular plates, exact solutions based on the theory of elasticity are only limited to thick plates with four simply supported edges [8–10]. Recently, Batra and Aimmanee [11] pointed out missing frequencies in the exact solutions of four simply supported edges rectangular plates obtained by Srinivas et al. [8].

Generally, approximating analytical and/or numerical methods based on the theory of elasticity are applied to solve 3-D free vibration of thick rectangular plates having arbitrary boundary conditions. Attempts at free vibration analysis of thick rectangular plates with various boundary conditions have been carried out. Sundara Raja Iyengar and Raman [12,13] analyzed frequencies of thick plates with simply supported and clamped edges using the method of initial function. Malik and Bert [14] analyzed the free vibration of thick rectangular plates using the differential quadrature method with the Levy technique. Liew and Teo [15] and Liew et al. [16] used the differential quadrature and harmonic differential quadrature methods, respectively to analyze the free vibration of rectangular plates. Filipich et al. [17] proposed a whole element method, which was used by the extended Fourier series techniques and analyzed free vibrations of rectangular plates. Hutchinson and Zillimer [18] and Fromme and Leissa [19] used the series method to analyze free vibrations of completely stress free rectangular parallelepiped.

The finite element method based on the theory of elasticity is well known and established as the most powerful and versatile application for solutions to 3-D free vibration problems of thick rectangular plates. However, the computing costs involved are often very large. On the other hand, semi-numerical methods such as the finite prism method [20] and the spline prism method [21] have also been used to analyze free vibrations of thick rectangular plates with one pair of parallel simply supported edges. Cheung and Chakrabarti [22] analyzed free vibration of thick rectangular plates with various boundary conditions using the finite layer method. Zhou et al. [23] also analyzed free vibration of thick rectangular plates with point supports using the finite layer method. Zhou et al. [23] used a new set of two types of basic functions in the plane direction, which are constructed with a one type being a set of static beam functions under sinusoidal load, and the other is for beam functions under point loads. Recently, Houmat [24] developed the h and p version finite element method based on the pentahedral p-element to analyze the free vibration of various thick plates. Houmat [24] used the element's new hierarchical shape functions, which are expressed in terms of shifted Legendre orthogonal polynomials.

The Ritz method provides some special advantages such as high accuracy, small computational cost, and easy coding. In the Ritz method, upper bound approximate solutions are obtained by minimizing the total potential energy with respect to the coefficients of the Ritz trial functions. The Ritz trial function is chosen in the following manner: (1) satisfying the essential boundary conditions of the plate, but not necessary by the natural boundary conditions of the plate; (2) functional completeness; and (3) linear independence. Therefore, improvements in the efficiency depend greatly on the choice of the Ritz trial functions or admissible functions. There are a number of reports of applications of the Ritz method based on the 3-D theory of elasticity with global admissible functions to analyze free vibration problems of isotropic thick rectangular plates. Leissa and Zhang [25], McGee and Leissa [26], Itakura [27], Lim [28], and Suda et al. [29] used simple algebraic polynomials, and Liew et al. [30–33] used general orthogonal polynomials with the Gram-Schmidt process in the Ritz method with global admissible functions to analyze free vibrations of rectangular plates. Zhou et al. [34] reported free vibrations of thick rectangular plates using the Ritz method with global admissible functions comprising Chebyshev polynomials multiplied by a boundary function. Rapid convergence and high accuracy were obtained in the analysis. Recently, Zhou et al. [35] have also performed free vibration analysis of rectangular plates with mixed boundary conditions using the Ritz method and including the admissible functions based on the Chebyshev polynomials combined with the R-function method.

This paper presents 3-D free vibration analysis of isotropic rectangular plates with any thicknesses arbitrary boundary conditions using the B-spline Ritz method. The formulation of the proposed method is based on the theory of elasticity, the Ritz procedure, and the method of artificial spring. The amplitude displacement components as the Ritz trial functions are assumed by a triplicate series of B-spline functions, which are piecewise polynomials. The geometric boundary conditions are numerically satisfied by the method of artificial spring. To demonstrate the convergence and accuracy of the proposed method, several examples with various boundary conditions were solved, and the results are compared with other published solutions by exact and other numerical methods based on the theory of elasticity, classical and shear deformation plate theories.

Stable, rapid convergence and high accuracy are obtained by the present method. Furthermore, a detailed investigation of the effects of the thickness–length ratio and the aspect ratio on the frequency parameters and the mode shapes of cantilevered thick rectangular plates were also carried out. The results are shown in tabular forms, and may serve as benchmark data for 3-D finite element solutions and future developments in new numerical methods.

2. B-spline functions as displacement amplitude functions

The B-spline functions were first introduced by Schoenberg [36], and Curry and Schoenberg [37,38]. A summary of the algebraic algorithms can be found by Boor [39], and a brief summary of B-spline functions is shown below.

The knot rows $\{t_n\}$ of the real number in the one-dimensional (1-D) domain are defined as follows:

$$\{t_n\} = t_{-k+1} \leqslant t_{-k+2} \leqslant \cdots \leqslant t_{-1} \leqslant t_0 \leqslant t_1 \leqslant \cdots \leqslant t_n \leqslant t_{n+1} \leqslant \cdots \leqslant t_{n+k-2} \leqslant t_{n+k-1}. \tag{1}$$

The kth divided difference of $g_k(t;x)$ in $\{t_n\}$ is

$$\begin{aligned} g_k(t;x) &= (t-x)_+^{k-1} \\ &= \begin{cases} (t-x)^{k-1}, & t \geqslant x, \\ 0, & t < x, \end{cases} \end{aligned} \tag{2}$$

and the B-spline function $M_{j,k}(x)$ is defined by

$$M_{j,k}(x) = \frac{\{g_k(t_{j+1}, t_{j+2}, \ldots, t_{j+k}; x) - g_k(t_j, t_{j+1}, \ldots, t_{j+k-1}; x)\}}{(t_{j+k} - t_j)}. \tag{3}$$

The normalized B-spline function $N_{j,k}(x)$ with the degree of spline functions $(k-1)$ is also defined as

$$N_{j,k}(x) = (t_{j+k} - t_j) M_{j,k}(x), \tag{4}$$

where the normalized B-spline function has the following characteristics:

$$\begin{aligned} &N_{j,k}(x) = 0 && (x \leqslant t_j,\ x \geqslant t_{j+k}), \\ &\sum_{i=1}^{s+q-k-1} N_{i+q-k,k}(x) = 1 && (t_q < x < t_s,\ q < s), \\ &N_{j,k}(x) > 0 && (t_j < x < t_{j+k}). \end{aligned} \tag{5}$$

Using Boor's algorithm [39], the normalized B-spline function can be calculated with good numerical stability. The recurrence formula as defined by Boor [39] is

$$N_{j,k}(x) = \frac{t_{j+k} - x}{t_{j+k} - t_{j+1}} N_{j+1,k-1}(x) + \frac{x - t_j}{t_{j+k-1} - t_j} N_{j,k-1}(x), \tag{6}$$

in which

$$N_{j,1}(x) = \begin{cases} 1, & j = i, \\ 0, & j \neq i. \end{cases} \tag{7}$$

The pth-order derivative of the normalized B-spline function are expressed by

$$N_{j,k}^{(p)}(x) = (k-1) \left\{ \frac{N_{j,k-1}^{(p-1)}(x)}{t_{j+k-1} - t_j} - \frac{N_{j+1,k-1}^{(p-1)}(x)}{t_{j+k} - t_{j+1}} \right\}, \tag{8}$$

where if $p = 0$,

$$N_{j,k}^{(0)}(x) = N_{j,k}(x), \tag{9}$$

in which k is the order of spline functions.

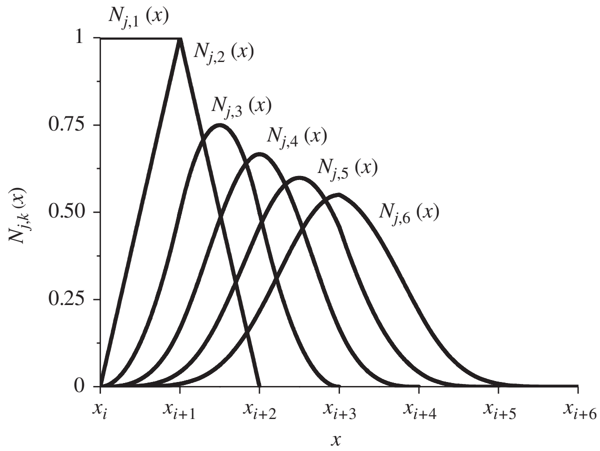

Fig. 1. Normalized B-spline functions $N_{j,k}(x)$ for varying k; $k = 1, 2,\ldots, 6$.

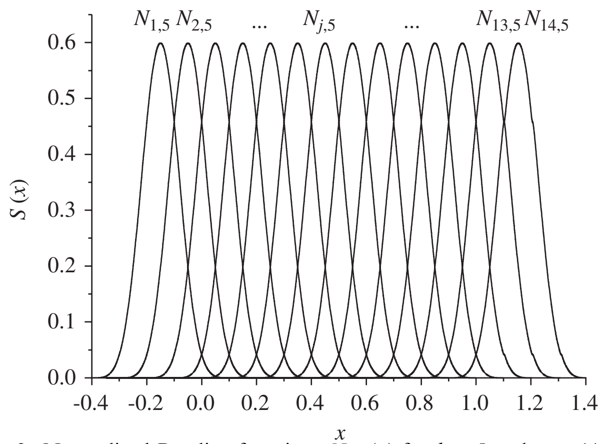

Fig. 2. Normalized B-spline functions $N_{j,5}(x)$ for $k = 5$ and $m = 11$.

An arbitrary function $S(x)$ can be expressed as the summation of a series of the normalized B-spline functions in the 1-D domain as follows:

$$S(x) = \sum_{n=1}^{N} A_n N_{n,k}(x), \tag{10}$$

where $N = m+k-2$; m is the number of knots, and $A_1, A_2, \ldots, A_n, \ldots, A_N$ are unknown spline coefficients, which are determined by the Ritz procedure. Here, $S(x)$ is a smooth piecewise polynomial up to the $(k-2)$th-order derivative. Fig. 1 gives the normalized B-spline functions $N_{j,k}(x)$ for varying the order of spline functions k and Fig. 2 depicts the normalized B-spline functions $N_{j,5}(x)$ for $m = 11$ and $k-1 = 4$.

3. Formulation the B-spline Ritz method and the governing eigenvalue equation

This section formulates the B-spline Ritz method by the linear and small strain 3-D theory of elasticity, and the Ritz procedure. The thick, homogeneous, and isotropic rectangular plate as outlined in Fig. 3 has a length a, a width b, and a uniform thickness h; the plate dimensions are defined with respect to a right-handed orthogonal coordinate system (x, y, z) and the plate domain is bounded by $0 \leqslant x \leqslant a$, $0 \leqslant y \leqslant b$, and $0 \leqslant z \leqslant h$. The stress free surfaces are assumed at $z = 0$ and h. The corresponding periodic displacement components at any point are defined by the in-plane components u, v, and the transverse component w in the x, y, and z directions, respectively.

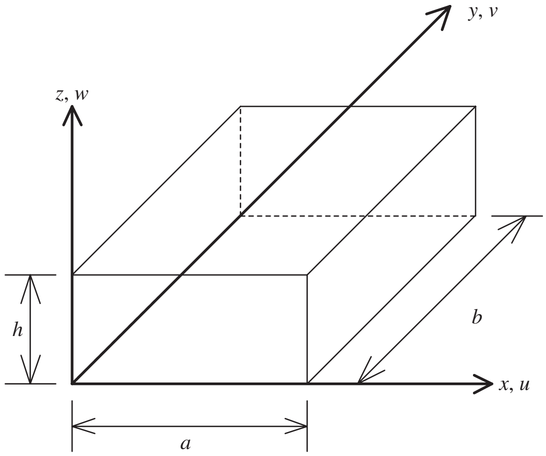

Fig. 3. Geometry, dimensions, and coordinates for an isotropic rectangular plate.

The strain energy $\overline{U}$ of an isotropic rectangular plate can be expressed in integral form as

$$\overline{U} = \frac{1}{2}\int_0^a \int_0^b \int_0^h (\Delta_1 \Gamma_1 + 2\Delta_2 \Gamma_2 + G\Gamma_3)\mathrm{d}z\,\mathrm{d}y\,\mathrm{d}x, \tag{11}$$

where

$$\Gamma_1 = \varepsilon_x^2 + \varepsilon_y^2 + \varepsilon_z^2, \quad \Gamma_2 = \varepsilon_x\varepsilon_y + \varepsilon_y\varepsilon_z + \varepsilon_z\varepsilon_x, \quad \Gamma_3 = \gamma_{xy}^2 + \gamma_{yz}^2 + \gamma_{zx}^2,$$
$$\Delta_1 = \frac{E(1-v)}{(1+v)(1-2v)}, \quad \Delta_2 = \frac{vE}{(1+v)(1-2v)}, \quad G = \frac{E}{2(1+v)}, \tag{12}$$

in which E is Young's modulus, v is Poisson's ratio, and G is shear modulus.

In 3-D theory of elasticity, the six generalized strain components in a right-handed orthogonal coordinate system are defined as

$$\varepsilon_x = \frac{\partial u}{\partial x}, \quad \varepsilon_y = \frac{\partial v}{\partial y}, \quad \varepsilon_z = \frac{\partial w}{\partial z}, \quad \gamma_{xy} = \frac{\partial u}{\partial y} + \frac{\partial v}{\partial x}, \quad \gamma_{yz} = \frac{\partial v}{\partial z} + \frac{\partial w}{\partial y}, \quad \gamma_{zx} = \frac{\partial w}{\partial x} + \frac{\partial u}{\partial z}. \tag{13}$$

Substituting Eq. (13) into Eq. (11), the strain energy $\overline{U}$ of the isotropic rectangular plate can be rewritten in integral and periodic displacement components u, v, w form as

$$\begin{aligned}
\overline{U} = \frac{1}{2}\int_0^a \int_0^b \int_0^h \Bigg[& \Delta_1 \left\{ \left(\frac{\partial u}{\partial x}\right)^2 + \left(\frac{\partial v}{\partial y}\right)^2 + \left(\frac{\partial w}{\partial z}\right)^2 \right\} \\
& + \Delta_2 \left\{ \begin{array}{l} \left(\frac{\partial u}{\partial x}\right)\left(\frac{\partial v}{\partial y}\right) + \left(\frac{\partial v}{\partial y}\right)\left(\frac{\partial u}{\partial x}\right) + \left(\frac{\partial u}{\partial x}\right)\left(\frac{\partial w}{\partial z}\right) + \left(\frac{\partial w}{\partial z}\right)\left(\frac{\partial u}{\partial x}\right) \\ + \left(\frac{\partial v}{\partial y}\right)\left(\frac{\partial w}{\partial z}\right) + \left(\frac{\partial w}{\partial z}\right)\left(\frac{\partial v}{\partial y}\right) \end{array} \right\} \\
& + G \Bigg\{ \left(\frac{\partial u}{\partial y}\right)^2 + \left(\frac{\partial u}{\partial y}\right)\left(\frac{\partial v}{\partial x}\right) + \left(\frac{\partial v}{\partial x}\right)\left(\frac{\partial u}{\partial y}\right) + \left(\frac{\partial v}{\partial x}\right)^2 \\
& + \left(\frac{\partial v}{\partial z}\right)^2 + \left(\frac{\partial v}{\partial z}\right)\left(\frac{\partial w}{\partial y}\right) + \left(\frac{\partial w}{\partial y}\right)\left(\frac{\partial v}{\partial z}\right) + \left(\frac{\partial w}{\partial y}\right)^2 \\
& + \left(\frac{\partial w}{\partial x}\right)^2 + \left(\frac{\partial w}{\partial x}\right)\left(\frac{\partial u}{\partial z}\right) + \left(\frac{\partial u}{\partial z}\right)\left(\frac{\partial w}{\partial x}\right) + \left(\frac{\partial u}{\partial z}\right)^2 \Bigg\} \Bigg] \mathrm{d}z\,\mathrm{d}y\,\mathrm{d}x.
\end{aligned} \tag{14}$$

The kinetic energy $\overline{T}$ of the plate can be written as

$$\overline{T} = \frac{1}{2}\rho \int_0^a \int_0^b \int_0^h \left\{ \left(\frac{\partial u}{\partial t}\right)^2 + \left(\frac{\partial v}{\partial t}\right)^2 + \left(\frac{\partial w}{\partial t}\right)^2 \right\} \mathrm{d}z\,\mathrm{d}y\,\mathrm{d}x, \tag{15}$$

in which ρ is the mass density per unit volume.

Here, for simplicity and convenience in mathematical formulation, the following non-dimensional coordinate systems are introduced as

$$\xi = \frac{x}{a}, \quad \eta = \frac{y}{b}, \quad \zeta = \frac{z}{h}. \tag{16}$$

For the plate as an elastic body undergoing free harmonic vibrations, the periodic displacement components can be expressed by the non-dimensional displacement amplitude functions U, V, and W in ξ, η, and ζ coordinates and the temporal coordinate t as

$$u(x,y,z,t) = aU(\xi,\eta,\zeta)\mathrm{e}^{\mathrm{i}\omega t}, \quad v(x,y,z,t) = aV(\xi,\eta,\zeta)\mathrm{e}^{\mathrm{i}\omega t}, \quad w(x,y,z,t) = aW(\xi,\eta,\zeta)\mathrm{e}^{\mathrm{i}\omega t}, \tag{17}$$

where ω denotes the circular frequency of the plate and $\mathrm{i} = \sqrt{-1}$ is an imaginary constant.

The assumed spatial displacement field is based on a separable assumption for displacement amplitude functions, and each of the functions are expressed as the summation of a triplicate series of B-spline functions as follows:

$$\begin{aligned}
U(\xi,\eta,\zeta) &= \sum_{m=1}^{i_\xi}\sum_{n=1}^{i_\eta}\sum_{r=1}^{i_\zeta} A_{mnr} N_{m,k_\xi}(\xi) N_{n,k_\eta}(\eta) N_{r,k_\zeta}(\zeta),\\
V(\xi,\eta,\zeta) &= \sum_{m=1}^{i_\xi}\sum_{n=1}^{i_\eta}\sum_{r=1}^{i_\zeta} B_{mnr} N_{m,k_\xi}(\xi) N_{n,k_\eta}(\eta) N_{r,k_\zeta}(\zeta),\\
W(\xi,\eta,\zeta) &= \sum_{m=1}^{i_\xi}\sum_{n=1}^{i_\eta}\sum_{r=1}^{i_\zeta} C_{mnr} N_{m,k_\xi}(\xi) N_{n,k_\eta}(\eta) N_{r,k_\zeta}(\zeta),
\end{aligned} \tag{18}$$

in which $N_{m,k_\xi}(\xi)$, $N_{n,k_\eta}(\eta)$, and $N_{r,k_\zeta}(\zeta)$ are 1-D normalized B-spline functions with the degree of spline functions (k_l–1, the index l stands for the ξ, η, and ζ directions), and A_{mnr}, B_{mnr}, and C_{mnr} are unknown spline coefficients. The parameters appearing in Eq. (18) are defined as: $i_\xi = M_\xi + k_\xi - 2$, $i_\eta = M_\eta + k_\eta - 2$, and $i_\zeta = M_\zeta + k_\zeta - 2$, where M_ξ, M_η, and M_ζ, and k_ξ, k_η, and k_ζ are the number of knots and the order of spline functions in the ξ, η, and ζ directions, respectively.

Substituting Eqs. (17) and (18) into Eqs. (14) and (15), the maximum strain energy $U_{\max}$ and maximum kinetic energy $T_{\max}$ of the plate can be written in a non-dimensional coordinate systems as

$$\begin{aligned}
U_{\max} = \frac{abhE}{2}\int_0^1\int_0^1\int_0^1 \Bigg[& \bar{\Delta}_1 \left\{ \left(\frac{\partial U}{\partial \xi}\right)^2 + \left(\frac{a}{b}\right)^2 \left(\frac{\partial V}{\partial \eta}\right)^2 + \left(\frac{a}{h}\right)^2 \left(\frac{\partial W}{\partial \zeta}\right)^2 \right\} \\
& + \overline{\Delta}_2 \left\{ \begin{aligned} & \left(\frac{a}{b}\right)\left[\left(\frac{\partial U}{\partial \xi}\right)\left(\frac{\partial V}{\partial \eta}\right) + \left(\frac{\partial V}{\partial \eta}\right)\left(\frac{\partial U}{\partial \xi}\right)\right] + \left(\frac{a}{b}\right)\left(\frac{a}{h}\right)\left[\left(\frac{\partial V}{\partial \eta}\right)\left(\frac{\partial W}{\partial \zeta}\right) + \left(\frac{\partial W}{\partial \zeta}\right)\left(\frac{\partial V}{\partial \eta}\right)\right] \\ & + \left(\frac{a}{h}\right)\left[\left(\frac{\partial W}{\partial \zeta}\right)\left(\frac{\partial U}{\partial \xi}\right) + \left(\frac{\partial U}{\partial \xi}\right)\left(\frac{\partial W}{\partial \zeta}\right)\right] \end{aligned} \right\} \\
& + \overline{\Delta}_3 \Bigg\{ \left(\frac{a}{b}\right)^2 \left(\frac{\partial U}{\partial \eta}\right) + \left(\frac{a}{b}\right)\left[\left(\frac{\partial U}{\partial \eta}\right)\left(\frac{\partial V}{\partial \xi}\right) + \left(\frac{\partial V}{\partial \xi}\right)\left(\frac{\partial U}{\partial \eta}\right)\right] + \left(\frac{\partial V}{\partial \xi}\right)^2 \\
& + \left(\frac{a}{h}\right)^2 \left(\frac{\partial V}{\partial \zeta}\right) + \left(\frac{a}{b}\right)\left(\frac{a}{h}\right)\left[\left(\frac{\partial V}{\partial \zeta}\right)\left(\frac{\partial W}{\partial \eta}\right) + \left(\frac{\partial W}{\partial \eta}\right)\left(\frac{\partial V}{\partial \zeta}\right)\right] + \left(\frac{a}{b}\right)^2 \left(\frac{\partial W}{\partial \eta}\right)^2
\end{aligned}$$

$$+\left(\frac{\partial W}{\partial \xi}\right)^2+\left(\frac{a}{h}\right)\left[\left(\frac{\partial W}{\partial \xi}\right)\left(\frac{\partial U}{\partial \zeta}\right)+\left(\frac{\partial U}{\partial \zeta}\right)\left(\frac{\partial W}{\partial \xi}\right)\right]+\left(\frac{a}{h}\right)^2\left(\frac{\partial U}{\partial \zeta}\right)^2\Bigg\}\Bigg]\mathrm{d}\zeta\,\mathrm{d}\eta\,\mathrm{d}\xi$$
$$=\frac{abhE}{2}\{\varDelta\}^{\mathrm{T}}_{mnr}[K]_{mnrijs}\{\varDelta\}_{ijs} \tag{19}$$

and

$$T_{\max}=\frac{\rho\omega^2 a^3 bh}{2}\int_0^1\int_0^1\int_0^1 (U^2+V^2+W^2)\mathrm{d}\zeta\,\mathrm{d}\eta\,\mathrm{d}\xi$$
$$=\frac{\rho\omega^2 a^3 bh}{2}\{\varDelta\}^{\mathrm{T}}_{mnr}[M]_{mnrijs}\{\varDelta\}_{ijs}, \tag{20}$$

where

$$\overline{\varDelta}_1=\frac{(1-v)}{(1+v)(1-2v)},\quad \overline{\varDelta}_2=\frac{v}{(1+v)(1-2v)},\quad \overline{\varDelta}_3=\frac{1}{2(1+v)}. \tag{21}$$

$[K]_{mnrijs}$ and $[M]_{mnrijs}$ are the stiffness and mass matrices, respectively, and $\{\varDelta\}_{ijs}$ is the unknown coefficient vector in the following:

$$\{\varDelta\}_{ijs}=\{\{\delta_A\}\{\delta_B\}\{\delta_C\}\}^{\mathrm{T}}, \tag{22}$$

in which the column vectors $\{\delta_A\}$, $\{\delta_B\}$, and $\{\delta_C\}$ are composed by the unknown spline coefficients in Eq. (18) as

$$\{\delta_A\}=\{A_{111}A_{112}\ldots A_{11i_\zeta}A_{121}\ldots A_{12i_\zeta}\ldots A_{1i_\eta i_\zeta}\ldots A_{i_\xi i_\eta i_\zeta}\}^{\mathrm{T}},$$
$$\{\delta_B\}=\{B_{111}B_{112}\ldots B_{11i_\zeta}B_{121}\ldots B_{12i_\zeta}\ldots B_{1i_\eta i_\zeta}\ldots B_{i_\xi i_\eta i_\zeta}\}^{\mathrm{T}},$$
$$\{\delta_C\}=\{C_{111}C_{112}\ldots C_{11i_\zeta}C_{121}\ldots C_{12i_\zeta}\ldots C_{1i_\eta i_\zeta}\ldots C_{i_\xi i_\eta i_\zeta}\}^{\mathrm{T}}. \tag{23}$$

The boundary conditions at the four edges ($x=0$, a and $y=0$, b) of a thick rectangular plate would be satisfied as follows:

(a) Simply supported

$$v=w=0,\quad \sigma_x=0\quad \text{at } x=0,a,$$
$$u=w=0,\quad \sigma_y=0\quad \text{at } y=0,b. \tag{24}$$

(b) Clamped edge

$$u=v=w=0\quad \text{at } x=0,a,$$
$$u=v=w=0\quad \text{at } y=0,b. \tag{25}$$

(c) Free edge (stress free edge)

$$\sigma_x=\tau_{xy}=\tau_{xz}=0\quad \text{at } x=0,a,$$
$$\sigma_y=\tau_{yx}=\tau_{yz}=0\quad \text{at } y=0,b. \tag{26}$$

The boundary conditions for the top and bottom stress free surfaces of the plate can be expressed by

$$\sigma_z=\tau_{zy}=\tau_{zx}=0\quad \text{at } z=0,h. \tag{27}$$

In the Ritz method, it is sufficient to choose displacement amplitude functions as trial functions that satisfy only the essential boundary conditions of the plate. The natural boundary conditions are included in the variational statement. Hence, there is no need to explicitly satisfy the natural boundary conditions of the trial function. However, in Eq. (18), the normalized B-spline functions do not satisfy the essential boundary conditions. Therefore, the general treatment of the essential boundary conditions has to be considered greatly.

To deal with the geometric boundary conditions at the four edges ($x=0$, a and $y=0$, b), the method of artificial spring [40] is used. In this method, three types of spring coefficients α, β, and γ corresponding to the geometric boundary conditions u, v, and w are introduced at each boundary edges of the plate.

The energy contribution L due to the springs is given by

$$L=\frac{1}{2}\int_0^b\int_0^h(\alpha u^2+\beta v^2+\gamma w^2)\,\mathrm{d}z\,\mathrm{d}y\bigg|_{x=0,a}+\frac{1}{2}\int_0^a\int_0^h(\alpha u^2+\beta v^2+\gamma w^2)\,\mathrm{d}z\,\mathrm{d}x\bigg|_{y=0,b}. \tag{28}$$

Substituting Eqs. (17) and (18) into Eq. (28), the maximum artificial spring energy $L_{\max}$ of the plate can be given in a non-dimensional coordinate systems as

$$\begin{aligned}L_{\max}&=\frac{abhE}{2}\left\{\begin{array}{l}\int_0^1\int_0^1(k_\alpha U^2+k_\beta V^2+k_\gamma W^2)\,\mathrm{d}\zeta\,\mathrm{d}\eta\Big|_{\xi=0,1}\\+\left(\frac{a}{b}\right)\int_0^1\int_0^1(k_\alpha U^2+k_\beta V^2+k_\gamma W^2)\,\mathrm{d}\zeta\,\mathrm{d}\xi\Big|_{\eta=0,1}\end{array}\right\}\\&=\frac{abhE}{2}\{\Delta\}^{\mathrm{T}}_{mnr}[K^L]_{mnrijs}\{\Delta\}_{ijs},\end{aligned} \tag{29}$$

$$k_\alpha=\frac{\alpha a}{E},\quad k_\beta=\frac{\beta a}{E},\quad k_\gamma=\frac{\gamma a}{E}, \tag{30}$$

where $[K^L]_{mnrijs}$ is the stiffness matrix for the artificial springs, and k_α, k_β, and k_γ are non-dimensional spring parameters.

For the geometric boundary conditions at the four edges ($\xi=0$, 1 and $\eta=0$, 1), the non-dimensional spring parameters k_α, k_β, and k_γ are assumed to be zero, and this results in the stress free boundary condition. If the spring parameter is assumed to be infinite, the boundary edges will lead to procedure the fixed condition. For example, chosen simply supported and clamped edges at $\xi=0$, 1 set the spring parameters become $k_\beta=k_\gamma=\infty$ and $k_\alpha=k_\beta=k_\gamma=\infty$, respectively. However, numerical computation cannot deal with infinite values, and the determination of the spring parameters is described in the next section.

The total potential energy Π of the isotropic plate can be expressed as

$$\Pi=(U_{\max}+L_{\max})-T_{\max}. \tag{31}$$

In Eq. (31), minimizing the total potential energy Π with respect to the unknown spline coefficient vectors $\{\Delta\}^{\mathrm{T}}_{mnr}$, i.e.:

$$\frac{\partial\Pi}{\partial\{\Delta\}^{\mathrm{T}}_{mnr}}=0, \tag{32}$$

which leads to the following governing eigenvalue equation in matrix form:

$$\left[\begin{array}{c}\left(\begin{bmatrix}[K_{UU}]&[K_{UV}]&[K_{UW}]\\ [K_{VU}]&[K_{VV}]&[K_{VW}]\\ [K_{WU}]&[K_{WV}]&[K_{WW}]\end{bmatrix}+\begin{bmatrix}[K^L_{UU}]&[0]&[0]\\ [0]&[K^L_{VV}]&[0]\\ [0]&[0]&[K^L_{WW}]\end{bmatrix}\right)\\ -n^{*2}\begin{bmatrix}[M_{UU}]&[0]&[0]\\ [0]&[M_{VV}]&[0]\\ [0]&[0]&[M_{WW}]\end{bmatrix}\end{array}\right]\begin{Bmatrix}\{\delta_A\}\\ \{\delta_B\}\\ \{\delta_C\}\end{Bmatrix}=\begin{Bmatrix}\{0\}\\ \{0\}\\ \{0\}\end{Bmatrix}, \tag{33}$$

in which $n^*=\omega a\sqrt{\rho/E}$ is the frequency parameter; $[K_{IJ}]$, $[K^L_{II}]$, and $[M_{II}]$ (I, $J=U$, V and W) are, respectively, the sub-stiffness matrices, the diagonal sub-stiffness matrices of artificial spring, and the diagonal sub-mass matrices. In general, when the Ritz method with global admissible functions is used, the system matrix as stiffness and mass matrices will result in a full symmetric matrix. However, in the proposed method, the stiffness matrix $[K]_{mnrijs}$ is positive definite symmetric band form, and the mass matrix $[M]_{mnrijs}$ is also symmetric band form. The size of the matrix in Eq. (33) is $3\times(M_\xi+k_\xi-2)\times(M_\eta+k_\eta-2)\times(M_\zeta+k_\zeta-2)$. The general expressions for $[K_{IJ}]$, $[K^L_{II}]$, and $[M_{II}]$ are given in Appendix A. The numerical calculations of the eigenvalue used the Householder-QR method, and the mode shape corresponding to each eigenvalue can be obtained by an inverse iteration method. In the case of the plate having all stress free edges which has six rigid body modes, the stiffness matrix is not positive definite. Only in this case, the double-QR method is used in the calculations of the eigenvalue.

4. Numerical examples and discussions

The natural frequencies of isotropic rectangular plates with arbitrary boundary conditions are solved to illustrate the convergence of the solutions and the accuracy of the B-spline Ritz method. For the definition of the boundary conditions of the plate with stress free top and bottom surfaces, for example, the symbols SF-CS, identifies a plate with edges $\xi = 0$, 1 and $\eta = 0$, 1 having simply supported edge (S), stress free edge (F), clamped edge (C) and simply supported edge (S), respectively. The geometric parameters of the plate are defined by the thickness–length ratio h/a and the aspect ratio b/a. The numerical calculations use $v = 0.3$.

The vibration modes of the plate can be defined into at least two types, in which the displacement amplitude components U and V are symmetric distribution (namely symmetric modes, S), and U and V are anti-symmetric distribution (namely anti-symmetric modes, A) with respect to the ζ direction, respectively. Further, if the plate has one pair of parallel the symmetric boundary conditions in the ξ or η directions, then its typical vibration modes can be divided into the following four categories: S–S, S–A, A–S, and A–A, in which the first of the letters in the symbol pairs refer to the vibration mode in the ξ or η directions and the second letter to that for the middle surface ($\zeta = 0.5$). For the plate with symmetric boundary conditions in the ξ and η directions, the typical vibration modes can be divided into eight distinct categories: SS–S, SS–A, SA–S, SA–A, AS–S, AS–A, AA–S, and AA–A, where the three letters refer to the vibration modes in the ξ, η, and ζ directions, respectively. The supper scripts T, M, and t denote the thickness mode (anti-symmetric distribution W at the middle surface), the in-plane mode ($W = 0$ with one pair of parallel simply supported edges), and the torsional mode (anti-symmetric deformation W in the ξ or η direction with one pair of parallel stress free edges), respectively. Note that the membrane mode $U = W = 0$ and $V = W = 0$ are the missing vibration modes of four simply supported edges plate [11], which are not considered by Srinivas et al. [8].

The frequency parameter Ω^* of the plate is expressed as

$$\Omega^* = \omega b^2 \sqrt{\rho h/D}, \tag{34}$$

where $D = Eh^3/12(1-v^2)$ is the flexural rigidity of the plate.

All computations are preformed in double precision on a personal computer, and all of the frequency parameters and vibration modes are accurate up to five significant digits.

4.1. Determination of the non-dimensional spring parameters

Numerical computations cannot deal with infinite values, and the determination of the spring parameters is investigated in this sub-section. Table 1 shows the effect of the non-dimensional spring parameters $k_\alpha = k_\beta = k_\gamma$ on the convergence of the first eight frequency parameters Ω^* for SS–SS and CC–FF isotropic square plates ($b/a = 1$). The thickness–length ratios h/a are 0.001, 0.2, and 0.5 corresponding to very thin, moderately thick, and very thick plates. The degree of spline functions $(k_\xi-1) \times (k_\eta-1) \times (k_\zeta-1)$ are set as $5 \times 5 \times 2$ ($h/a = 0.001$) and $4 \times 4 \times 3$ ($h/a = 0.2$ and 0.5). The number of knots $M_\xi \times M_\eta \times M_\zeta$ is fixed as $21 \times 21 \times 3$ ($h/a = 0.001$) and $15 \times 15 \times 9$ ($h/a = 0.2$ and 0.5). Under these conditions, the spring parameters $k_\alpha = k_\beta = k_\gamma$ vary from 10^2 to 10^8. For a validation, the present results here are compared with other published results by using the 3-D exact solution [8], the 3-D Ritz solution with general orthogonal polynomials [30], the 3-D Ritz solution with Chebyshev polynomials [34], the exact solution based on the Mindlin plate theory [41], the Mindlin *pb*-2 Ritz solution [42], and the exact solution based on the classical thin plate theory [43]. All results of the Mindlin plate theory [41,42] were calculated using the shear correction factor $\kappa^2 = 5/6$. Similarly, the effect of the non-dimensional spring parameters $k_\alpha = k_\beta = k_\gamma$ on the convergence of the first eight frequency parameters Ω^* for SS–SS isotropic rectangular plates are also given in Table 2. The thickness–length ratio $h/a = 0.2$ is considered, and aspect ratio b/a are set as 0.5 and 2.

Table 1
Effect of the non-dimensional spring parameters $k_\alpha = k_\beta = k_\gamma$ on the convergence of the first eigth frequency parameters Ω^* for SS–SS and CC–FF square plates

Boundary conditions	h/a	$k_\alpha = k_\beta = k_\gamma$	Modes							
			1st	2nd	3rd	4th	5th	6th	7th	8th
SS–SS	0.001		SS–A	SA–A	AS–A	AA–A	SS–A	SS–A	SA–A	AS–A
		10^2	19.739	49.346	49.346	78.952	98.692	98.693	128.30	128.30
		10^4	19.740	49.347	49.347	78.954	98.694	98.694	128.30	128.30
		10^6	19.740	49.348	49.348	78.956	98.695	98.695	128.30	128.30
		10^8	19.741	49.348	49.349	78.956	98.695	98.695	128.30	128.30
	3-D Ritz [34]		19.712	49.347	49.347	78.953	98.691	98.691	128.30	128.30
	Mindlin-exact [41]		19.739	49.348	49.348	78.956	98.694	98.694	128.30	128.30
	CPT-exact [43]		19.739	49.348	49.348	78.957	98.696	98.696	128.30	128.30
	0.2		SS–A	SA–S^M	AS–S^M	SA–A	AS–A	SS–S^M	AA–A	AA–S^M
		10^2	17.430	31.827	31.827	38.306	38.306	45.526	55.449	63.651
		10^4	17.525	32.188	32.188	38.481	38.481	45.526	55.784	64.376
		10^6	17.526	32.192	32.192	38.483	38.483	45.526	55.787	64.383
		10^8	17.526	32.192	32.192	38.483	38.483	45.526	55.787	64.383
	3-D Ritz [30]		17.526	32.192	32.192	38.483	38.483	45.526	55.787	64.383
	3-D Ritz [34]		17.526	32.192	32.192	38.483	38.483	45.527	55.787	64.383
	3-D exact [8]		17.525	*	*	38.483	38.483	45.527	55.790	*
	0.5		SS–A	SA–S^M	AS–S^M	SS–S^M	SA–A	AS–A	AA–S^M	AA–S^M
		10^2	12.346	12.731	12.731	18.210	22.863	22.863	25.461	25.465
		10^4	12.425	12.875	12.875	18.210	23.006	23.006	25.750	25.750
		10^6	12.426	12.877	12.877	18.210	23.008	23.008	25.753	25.753
		10^8	12.426	12.877	12.877	18.210	23.008	23.008	25.753	25.753
	3-D Ritz [30]		12.426	12.877	12.877	18.210	23.008	23.008	25.754	25.754
	3-D Ritz [34]		12.426	12.877	12.877	18.210	23.008	23.008	25.754	25.754
	3-D exact [8]		12.426	*	*	18.210			*	*
CC–FF	0.001		SS–A	SA–A^T	SS–A	AS–A	AA–A^T	SA–A^T	AS–A	SS–A
		10^2	21.267	25.505	42.748	58.766	64.783	79.090	85.226	115.52
		10^4	22.159	26.396	43.584	61.151	67.148	79.805	87.566	120.05
		10^6	22.204	26.442	43.629	61.276	67.274	79.845	87.694	120.30
		10^8	22.211	26.449	43.636	61.295	67.293	79.851	87.713	120.34
	Mindlin–Ritz [42]		22.181	26.427	43.614	61.195	67.223	79.825	87.627	120.14
	CPT-exact [43]		22.272	26.529	43.664	61.466	67.549	79.904		
	0.2		SS–A	SA–A^T	SA–$S^{T,\ T}$	SS–A	AS–A	AA–A^T	AS–S^T	SA–A^T
		10^2	17.187	19.601	29.022	31.191	39.590	42.657	51.510	53.252
		10^4	17.752	20.090	29.376	31.489	40.512	43.496	52.603	53.613
		10^6	17.759	20.096	29.380	31.492	40.524	43.507	52.615	53.615
		10^8	17.760	20.096	29.380	31.492	40.524	43.507	52.615	53.615
	3-D Ritz [30]		17.761	20.097	29.382	31.493	40.527	43.509	52.618	53.617
	0.5		SS–A	SA–A^T	SA–$S^{T,\ T}$	SS–A	AS–A	AS–S^T	AA–$S^{T,\ T}$	AA–A^T
		10^2	10.387	11.306	11.625	18.393	20.462	20.694	21.403	22.285
		10^4	10.579	11.447	11.768	18.465	20.680	21.132	21.639	22.500
		10^6	10.582	11.448	11.769	18.466	20.682	21.137	21.641	22.502
		10^8	10.582	11.448	11.769	18.466	20.682	21.137	21.641	22.502
	3-D Ritz [30]		10.583	11.450	11.770	18.466	20.684	21.140	21.642	22.504

*are missing frequencies [11].

Tables 1 and 2 show that good convergence and accuracy of the solutions are obtained by increasing the spring parameters for all cases. It is seen that good results from very thin plates to thick plates are obtained by using $k_\alpha = k_\beta = k_\gamma = 10^6$.

Table 2
Effect of the non-dimensional spring parameters $k_\alpha = k_\beta = k_\gamma$ on the convergence of the first eigth frequency parameters Ω^* for SS–SS rectangular plates with $h/a = 0.2$

b/a	$k_\alpha = k_\beta = k_\gamma$	Modes							
		1st	2nd	3rd	4th	5th	6th	7th	8th
0.5		SA–S^M	SS–A	AS–A	AS–S^M	AA–S^M	SS–S^M	SS–A	AS–S^M
	10^2	7.9270	9.5478	13.821	15.795	15.855	17.850	19.805	22.763
	10^4	8.0467	9.6199	13.945	16.093	16.093	17.994	19.966	22.763
	10^6	8.0479	9.6207	13.947	16.096	16.096	17.996	19.968	22.763
	10^8	8.0479	9.6207	13.947	16.096	16.096	17.996	19.968	22.763
	3-D Ritz [30]	8.0477	9.6209	13.947	16.096	16.096	17.995	19.967	22.763
2		SS–A	AS–S^M	SA–A	SS–A	SA–S^M	AA–S^M	AS–A	SS–S^M
	10^2	45.486	63.894	69.816	106.98	127.55	127.79	134.30	143.38
	10^4	45.618	64.379	70.101	107.37	128.75	128.76	134.66	143.96
	10^6	45.619	64.383	70.104	107.37	128.77	128.77	134.66	143.97
	10^8	45.619	64.383	70.104	107.37	128.77	128.77	134.66	143.97
	3-D Ritz [30]	45.619	64.383	70.104	107.37	128.77	128.77	134.66	143.97

Table 3
Effect of the degree of spline functions $(k_\xi-1) \times (k_\eta-1) \times (k_\zeta-1)$ and the number of knots $M_\xi \times M_\eta \times M_\zeta$ on the convergence of the first ten frequency parameters Ω^* for SS–SS square plates

h/a	$(k_\xi-1) \times (k_\eta-1) \times (k_\zeta-1)$	$M_\xi \times M_\eta \times M_\zeta$	dof	Modes									
				1st	2nd	3rd	4th	5th	6th	7th	8th	9th	10th
				SS–A	SA–A	AS–A	AA–A	SS–A	SS–A	SA–A	AS–A	SA–S^M	AS–S^M
0.05	4 × 4 × 3	7 × 7 × 5	2100	19.569	48.312	48.312	76.362	94.825	94.825	121.79	121.79	128.77	128.77
		9 × 9 × 5	3024	19.569	48.310	48.310	76.360	94.706	94.706	121.70	121.70	128.77	128.77
		11 × 11 × 5	4116	19.569	48.310	48.310	76.360	94.699	94.699	121.69	121.69	128.77	128.77
	4 × 4 × 3	7 × 7 × 7	2700	19.569	48.312	48.312	76.362	94.825	94.825	121.79	121.79	128.77	128.77
		9 × 9 × 7	3888	19.569	48.310	48.310	76.360	94.706	94.706	121.70	121.70	128.77	128.77
		11 × 11 × 7	5292	19.569	48.310	48.310	76.360	94.699	94.699	121.69	121.69	128.77	128.77
	5 × 5 × 3	7 × 7 × 5	2541	19.569	48.310	48.310	76.360	94.713	94.713	121.70	121.70	128.77	128.77
		9 × 9 × 5	3549	19.569	48.310	48.310	76.360	94.699	94.699	121.69	121.69	128.77	128.77
		11 × 11 × 5	4725	19.569	48.310	48.310	76.360	94.698	94.698	121.69	121.69	128.77	128.77
	Mizusawa and Takagi [21]		–	19.569	48.310	48.310	76.360	94.698	94.698	121.69	121.69	128.77	128.77
				SS–A	SA–S^M	AS–S^M	SS–S^M	SA–A	AS–A	AA–S^M	AA–S^M	AA–A	SA–S^M
0.3	4 × 4 × 3	7 × 7 × 7	2700	15.688	21.461	21.461	30.351	31.984	31.984	42.922	42.922	44.534	47.989
		9 × 9 × 7	3888	15.688	21.461	21.461	30.351	31.984	31.984	42.922	42.922	44.534	47.989
		11 × 11 × 7	5292	15.688	21.461	21.461	30.351	31.984	31.984	42.922	42.922	44.534	47.989
	4 × 4 × 3	7 × 7 × 9	3300	15.688	21.461	21.461	30.351	31.984	31.984	42.922	42.922	44.534	47.989
		9 × 9 × 9	4752	15.688	21.461	21.461	30.351	31.984	31.984	42.922	42.922	44.534	47.989
		11 × 11 × 9	6468	15.688	21.461	21.461	30.351	31.984	31.984	42.922	42.922	44.534	47.989
	5 × 5 × 3	7 × 7 × 7	3267	15.688	21.461	21.461	30.351	31.984	31.984	42.922	42.922	44.534	47.989
		9 × 9 × 7	4563	15.688	21.461	21.461	30.351	31.984	31.984	42.922	42.922	44.534	47.989
		11 × 11 × 7	6075	15.688	21.461	21.461	30.351	31.984	31.984	42.922	42.922	44.534	47.989
	Mizusawa and Takagi [21]		–	15.688	21.461	21.461	30.351	31.984	31.984	42.922	42.922	44.534	47.989
				SS–A	SA–S^M	AS–S^M	SS–S^M	SA–A	AS–A	AA–S^M	AA–S^M	SA–A^M	AS–A^M
0.5	4 × 4 × 3	7 × 7 × 9	3300	12.426	12.877	12.877	18.210	23.008	23.008	25.753	25.753	28.793	28.793
		9 × 9 × 9	4752	12.426	12.877	12.877	18.210	23.008	23.008	25.753	25.753	28.793	28.793
		11 × 11 × 9	6468	12.426	12.877	12.877	18.210	23.008	23.008	25.753	25.753	28.793	28.793
	5 × 5 × 3	7 × 7 × 9	3993	12.426	12.877	12.877	18.210	23.008	23.008	25.753	25.753	28.793	28.793
		9 × 9 × 9	5577	12.426	12.877	12.877	18.210	23.008	23.008	25.753	25.753	28.793	28.793
		11 × 11 × 9	7425	12.426	12.877	12.877	18.210	23.008	23.008	25.753	25.753	28.793	28.793
	Mizusawa and Takagi [21]		–	12.426	12.877	12.877	18.210	23.008	23.008	25.753	25.753	28.793	28.793

Based on the results obtained in this sub-section, the non-dimensional spring parameters $k_\alpha = k_\beta = k_\gamma = 10^6$ are used in the following analysis.

4.2. Convergence and comparison studies

The Ritz method provides theoretically accurate solutions, and, generally, the natural frequencies obtained by the Ritz procedure are the upper bounds of the exact frequencies. The convergence behaviors are monotonic from above as the number of terms of the global admissible functions increase. On the other hand, convergence of the present method is determined by the degree of spline functions $(k_\xi-1)\times(k_\eta-1)\times(k_\zeta-1)$ and the number of knots $M_\xi \times M_\eta \times M_\zeta$. In 3-D free vibration analysis of the plate, the significant digits and computational capacity will inevitably result in limitations to the triplicate series used. In some problems, high-order vibration frequencies must be determined for the practical applications. For instance when structural components such as plates are subjected to impact loads, it is necessary to investigate a high-order vibration modes to provide a realistic prediction for the dynamic response analysis. Therefore, it is important to investigate (1) the effects of the degree of spline functions and the number of knots on the convergence of the present method, and (2) the accuracy of the present method with low- and high-order vibration frequencies.

Table 4
Effect of the degree of spline functions $(k_\xi-1)\times(k_\eta-1)\times(k_\zeta-1)$ and the number of knots $M_\xi \times M_\eta \times M_\zeta$ on the convergence of high-order frequencies parameters Ω^* for SS–SS square plates

h/a	$(k_\xi-1)\times(k_\eta-1)\times(k_\zeta-1)$	$M_\xi \times M_\eta \times M_\zeta$	Modes										
			15th	20th	30th	40th	50th	60th	70th	80th	90th	100th	150th
			AA–A	SS–A	SS–S^T	AS–A	SA–A	AA–S^M	AA–A	SS–A	SS–S^M	AS–A	SS–S^M
0.05	4 × 4 × 3	15 × 15 × 5	182.48	232.37	307.70	386.30	436.75	515.07	564.79	632.30	656.59	722.40	920.18
		17 × 17 × 5	182.48	232.36	307.70	386.30	436.59	515.07	564.76	629.10	656.58	719.74	912.42
		19 × 19 × 5	182.48	232.36	307.70	386.30	436.56	515.07	564.76	628.46	656.58	719.20	910.52
	4 × 4 × 3	15 × 15 × 7	182.48	232.37	307.70	386.30	436.74	515.07	564.79	632.30	656.59	722.40	920.18
		17 × 17 × 7	182.48	232.36	307.70	386.30	436.59	515.07	564.76	629.10	656.58	719.74	912.42
	5 × 5 × 3	15 × 15 × 5	182.48	232.36	307.70	386.30	436.56	515.07	564.76	629.12	656.58	719.75	919.05
		17 × 17 × 5	182.48	232.36	307.70	386.30	436.54	515.07	564.75	628.35	656.58	719.11	910.52
		19 × 19 × 5	182.48	232.36	307.70	386.30	436.54	515.07	564.75	628.24	656.58	719.02	910.52
	Mizusawa and Takagi [21]		182.48	232.36	307.70	386.30	436.54	515.07	564.75	628.22	656.59	718.99	910.52
			AA–S^M	SS–S^M	SA–S^M	SA–S^M	AA–S^M	AS–S^T	AS–A	SA–A^M	AA–A	AA–A	SA–S^M
0.3	4 × 4 × 3	11 × 11 × 7	60.701	67.866	77.379	88.487	95.978	105.01	108.76	113.79	119.63	123.69	144.06
		13 × 13 × 7	60.701	67.866	77.379	88.487	95.977	105.01	108.76	113.79	119.57	123.69	143.98
		15 × 15 × 7	60.701	67.866	77.379	88.487	95.977	105.01	108.76	113.79	119.56	123.69	143.97
	4 × 4 × 3	11 × 11 × 9	60.701	67.866	77.379	88.487	95.978	105.01	108.76	113.79	119.63	123.69	144.06
		13 × 13 × 9	60.701	67.866	77.379	88.487	95.977	105.01	108.76	113.79	119.57	123.69	143.98
		15 × 15 × 9	60.701	67.866	77.379	88.487	95.977	105.01	108.76	113.79	119.56	123.69	143.97
	5 × 5 × 3	11 × 11 × 7	60.701	67.866	77.379	88.487	95.977	105.01	108.76	113.79	119.57	123.69	143.98
		13 × 13 × 7	60.701	67.866	77.379	88.487	95.977	105.01	108.76	113.79	119.56	123.69	143.97
		15 × 15 × 7	60.701	67.866	77.379	88.487	95.977	105.01	108.76	113.79	119.56	123.69	143.97
	Mizusawa and Takagi [21]		60.701	67.866	77.379	88.487	95.977	105.01	108.76	113.79	119.56	123.69	143.97
			SS–A^M	AA–S^M	SS–S^M	SA–S^M	AA–A	SA–S^T	AA–A^M	AS–A^M	AA–A^M	SS–A	SA–A
0.5	4 × 4 × 3	11 × 11 × 9	31.541	36.421	40.720	46.428	51.598	53.586	57.587	59.009	63.083	64.547	75.583
		13 × 13 × 9	31.541	36.421	40.720	46.428	51.598	53.585	57.586	59.009	63.083	64.547	75.580
		15 × 15 × 9	31.541	36.421	40.720	46.428	51.598	53.585	57.586	59.009	63.083	64.547	75.579
	5 × 5 × 3	11 × 11 × 9	31.541	36.421	40.720	46.428	51.598	53.585	57.586	59.009	63.083	64.547	75.580
		13 × 13 × 9	31.541	36.421	40.720	46.428	51.598	53.585	57.586	59.009	63.083	64.547	75.579
	Mizusawa and Takagi [21]		31.541	36.421	40.720	46.428	51.598	53.585	57.586	59.008	63.083	64.546	75.578

Table 3 shows the effects of the degree of spline functions $(k_\xi-1)\times(k_\eta-1)\times(k_\zeta-1)$ and the number of knots $M_\xi\times M_\eta\times M_\zeta$ on the convergence of the first ten frequency parameters Ω^* for SS–SS square plates ($b/a=1$). The thickness–length ratio h/a are set as 0.05, 0.3 and 0.5. The number of knots in the thickness direction M_ζ fixed as 5 and 7 for $h/a=0.05$, 7 and 9 for $h/a=0.3$, and 9 for $h/a=0.5$. The number of knots in the in-plane $M_\xi\times M_\eta$ varied from 5×5 to 15×15, while the degree of spline functions $(k_\xi-1)\times(k_\eta-1)\times(k_\zeta-1)$ are set as $4\times4\times3$ and $5\times5\times3$. Degrees of freedom (dof) means the size of matrix of the present method. Similarly, high-order frequencies parameters Ω^* used to evaluate the convergence study is also shown in Table 4, giving the 15th, 20th, 30th, 40th, 50th, 60th, 70th, 80th, 90th, 100th, and 150th modes. For comparison of the results, the spline prism method by Mizusawa and Takagi [21] are used to calculate frequency parameters. The results are listed in Tables 3 and 4.

Tables 3 and 4 show that stable convergence can be obtained by increasing the number of knots $M_\xi\times M_\eta\times M_\zeta$ from thin plates to thick plates. It is found that frequency parameters rapidly converge up to the 100th modes by using the $5\times5\times3$ degree of spline functions, and a fixed $M_\xi\times M_\eta=15\times15$ and a minimum of $M_\zeta=7$ and/or 9 is necessary to obtain the convergence for first 100th frequencies in all the cases here (Table 4).

For a plate with clamped edges, it is well known that good results can be obtained by arranging discrete points closely near the clamped edges. The effects of the knot spacing patterns on the convergence of the first ten frequency parameters Ω^* for CC–CC isotropic square plates ($h/a=0.01$, 0.1, 0.4, and $b/a=1$) are shown by Tables 5–7. Three types spacing patterns in the ξ, η, and ζ directions are used as follows:

(a) a uniform spacing pattern: termed uniform distribution below:

$$\Theta_m=\frac{m-1}{M_\Theta-1}\quad\text{for } m=1,2,\ldots,M_\Theta, \tag{35}$$

(b) a non-uniform spacing pattern by the shifted Chebyshev–Gauss–Lobatto points [44]: termed shifted Chebyshev distribution below:

$$\Theta_m 0.5\left\{1-\cos\left(\frac{m-1}{M_\Theta-1}\pi\right)\right\},\quad m=1,2,\ldots,M_\Theta, \tag{36}$$

(c) a non-uniform spacing pattern by zeros of $(M_\Theta-2)$ th the shifted Legendre polynomials [45]: termed shifted Legendre distribution below:

$$\Theta_m=0.5(1+\overline{\Theta}_{m-1})\quad\text{for } m=2,\ldots,M_\Theta-1,\quad \Theta_1=0\quad\text{and}\quad\Theta_{M_\Theta}=1, \tag{37}$$

in which $\Theta=\xi$, η, ζ, and $\overline{\Theta}_{m-1}$'s are the Legendre polynomial zero roots defined by [−1, 1], which are well known Gauss–Legendre integral points. The spacing patterns for $M_\Theta=7$ and 13 are depicted in Fig. 4. It is seen that shifted Chebyshev distribution and shifted Legendre distribution are arranged closely near the edges. For validation, the present results are compared with other published solutions by the general orthogonal polynomials–Ritz method [30] and the Chebyshev polynomials–Ritz method [34]. The degree of spline functions $(k_\xi-1)\times(k_\eta-1)\times(k_\xi-1)$ are set as $3\times3\times2$, $4\times4\times2$ ($h/a=0.01$), and $3\times3\times3$, $4\times4\times3$ ($h/a=0.1$ and 0.4). The number of knots in the thickness direction M_ζ are fixed as 5 for $h/a=0.01$, 7 for $h/a=0.1$, and 9 for $h/a=0.4$. The number of knots $M_\xi\times M_\eta$ varies from 3×3 to 23×23.

The results calculated by the non-uniform spacing pattern with a relatively low-order degree of spline functions are more stable and rapidly obtained as shown in Tables 5–7. The convergence of the results calculated by the shifted Legendre distribution is slightly more rapid than that with the shifted Chebyshev distribution. However, the differences are not large.

Henceforth, the degree of spline functions $(k_\xi-1)\times(k_\eta-1)\times(k_\zeta-1)$ are set to $4\times4\times2$ for $h/a\leqslant0.05$ and $4\times4\times3$ for $h/a\geqslant0.1$. The number of knots $M_\xi\times M_\eta\times M_\zeta$ uses $15\times15\times5$ for $h/a\leqslant0.05$, $13\times13\times7$ for $0.1\leqslant h/a\leqslant0.3$, and $13\times13\times9$ for $h/a>0.3$, and the shifted Chebyshev distribution spacing pattern is used for rectangular plates with clamped edges in future numerical examples.

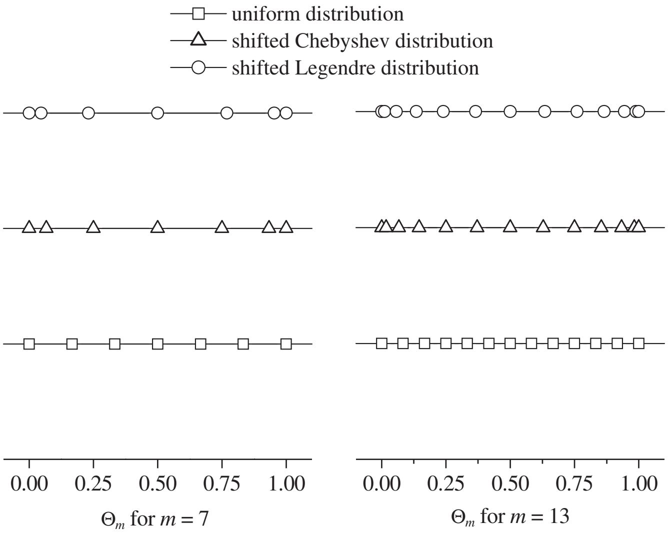

Fig. 4. Spacing patterns.

Table 5
Effect of knot spacing patterns on the convergence of the first ten frequency parameters Ω^* for CC–CC thin square plates with $h/a = 0.01$

Spacing pattern	$(k_\xi-1)\times(k_\eta-1)\times(k_\zeta-1)$	$M_\xi \times M_\eta \times M_\zeta$	Modes									
			1st SS–A	2nd SA–A	3rd AS–A	4th AA–A	5th SS–A	6th SS–A	7th SA–A	8th AS–A	9th SA–A	10th AS–A
Uniform distribution	3 × 3 × 2	7 × 7 × 5	36.563	78.173	78.173	113.94	177.39	178.15	204.13	204.13	274.34	492.57
		11 × 11 × 5	36.227	73.967	73.967	108.90	134.08	134.75	167.00	167.00	222.30	223.86
		15 × 15 × 5	36.140	73.660	73.660	108.51	132.05	132.68	165.36	165.36	211.84	211.84
		19 × 19 × 5	36.095	73.555	73.555	108.36	131.73	132.36	165.04	165.04	210.58	210.58
		23 × 23 × 5	36.066	73.495	73.495	108.27	131.60	132.23	164.89	164.89	210.26	210.26
	4 × 4 × 2	7 × 7 × 5	36.200	73.887	73.887	108.75	138.33	139.08	169.94	169.94	225.91	251.08
		11 × 11 × 5	36.093	73.547	73.547	108.35	131.75	132.38	165.05	165.05	211.35	211.35
		15 × 15 × 5	36.049	73.459	73.459	108.22	131.53	132.16	164.81	164.81	210.14	210.14
		19 × 19 × 5	36.025	73.410	73.410	108.15	131.44	132.07	164.70	164.70	209.97	209.97
Shifted Chebyshev distribution	3 × 3 × 2	7 × 7 × 5	37.518	90.133	90.133	129.09	232.90	233.68	256.75	256.75	346.38	579.70
		11 × 11 × 5	36.098	74.814	74.814	109.63	145.17	145.92	175.55	175.55	233.77	277.74
		15 × 15 × 5	35.996	73.500	73.500	108.20	133.26	133.92	165.97	165.97	220.95	221.81
		19 × 19 × 5	35.974	73.333	73.333	108.02	131.59	132.23	164.70	164.70	211.93	211.93
		23 × 23 × 5	35.966	73.297	73.297	107.98	131.31	131.94	164.49	164.49	210.16	210.16
Shifted Legendre distribution	3 × 3 × 2	7 × 7 × 5	38.025	95.521	95.521	136.39	264.53	265.25	287.35	287.35	388.97	647.19
		11 × 11 × 5	36.099	75.216	75.216	110.06	148.82	149.59	178.57	178.57	237.91	292.61
		15 × 15 × 5	35.986	73.520	73.520	108.21	133.72	134.39	166.29	166.29	221.36	224.55
		19 × 19 × 5	35.968	73.327	73.327	108.01	131.65	132.28	164.73	164.73	212.39	212.39
		23 × 23 × 5	35.964	73.293	73.293	107.97	131.31	131.95	164.48	164.48	210.24	210.24
	Liew et al. [30]		36.016	73.382	73.382	108.10	131.41	132.05	164.64	164.64	209.89	209.89

There are reports on 3-D free vibration analysis of isotropic rectangular plates having four simply supported edges (SS–SS) and four clamped edges (CC–CC). However, there are also some reports on 3-D free vibration analysis of cantilevered (CF–FF) and four stress free edges (FF–FF) rectangular plates based on the theory of elasticity. Therefore, the solutions obtained by the present method are presented in tabular form to serve as a validation.

Tables 8 and 9 give the first ten frequency parameters Ω^* for SS–SS and CC–CC square plates ($b/a = 1$) for thickness–length ratios h/a from 0.01 to 0.5. The $h/a = 0.01$, $h/a = 0.1, 0.2, 0.3$, and $h/a = 0.4, 0.5$ corresponds

Table 6
Effect of knot spacing patterns on the convergence of the first ten frequency parameters Ω* for CC–CC moderately thick square plates with $h/a = 0.1$

Spacing pattern	$(k_\xi-1)\times(k_\eta-1)\times(k_\zeta-1)$	$M_\xi\times M_\eta\times M_\zeta$	Modes									
			1st SS–A	2nd SA–A	3rd AS–A	4th AA–A	5th SS–A	6th SS–A	7th SA–S^T	8th SA–S^T	9th SA–A	10th AS–A
Uniform distribution	$3\times3\times3$	$7\times7\times7$	32.984	63.033	63.033	88.378	105.06	106.10	123.80	123.80	126.67	126.67
		$9\times9\times7$	32.899	62.838	62.838	88.138	104.00	105.00	123.70	123.70	125.81	125.81
		$11\times11\times7$	32.852	62.754	62.754	88.029	103.81	104.80	123.65	123.65	125.62	125.62
		$13\times13\times7$	32.824	62.704	62.704	87.965	103.72	104.71	123.62	123.62	125.53	125.53
		$15\times15\times7$	32.806	62.672	62.672	87.924	103.68	104.66	123.60	123.60	125.47	125.47
	$4\times4\times3$	$7\times7\times7$	32.889	62.818	62.818	88.113	103.98	104.98	123.69	123.69	125.77	125.77
		$9\times9\times7$	32.835	62.723	62.723	87.990	103.75	104.74	123.63	123.63	125.56	125.56
		$11\times11\times7$	32.806	62.674	62.674	87.926	103.68	104.67	123.60	123.60	125.47	125.47
		$13\times13\times7$	32.789	62.644	62.644	87.888	103.63	104.62	123.59	123.59	125.43	125.43
		$15\times15\times7$	32.778	62.625	62.625	87.863	103.61	104.59	123.58	123.58	125.39	125.39
Shifted Chebyshev distribution	$3\times3\times3$	$7\times7\times7$	32.840	63.322	63.322	88.596	109.09	110.20	123.63	123.63	129.61	129.61
		$9\times9\times7$	32.777	62.721	62.721	87.956	105.02	106.05	123.59	123.59	126.43	126.43
		$11\times11\times7$	32.758	62.608	62.608	87.837	103.86	104.85	123.56	123.56	125.56	125.56
		$13\times13\times7$	32.749	62.577	62.577	87.801	103.60	104.59	123.55	123.55	125.36	125.36
		$15\times15\times7$	32.743	62.564	62.564	87.785	103.53	104.52	123.55	123.55	125.31	125.31
Shifted Legendre distribution	$3\times3\times3$	$7\times7\times7$	32.822	63.652	63.652	88.957	110.62	111.75	123.61	123.61	130.84	130.84
		$9\times9\times7$	32.767	62.753	62.753	87.982	105.58	106.63	123.58	123.58	126.85	126.85
		$11\times11\times7$	32.753	62.606	62.606	87.831	103.98	104.98	123.56	123.56	125.64	125.64
		$13\times13\times7$	32.745	62.572	62.572	87.793	103.62	104.60	123.55	123.55	125.37	125.37
		$15\times15\times7$	32.741	62.560	62.560	87.779	103.53	104.52	123.55	123.55	125.30	125.30
	Zhou et al. [34]		32.743	62.562	62.562	87.783	103.51	104.49	123.55	123.55	125.29	125.29
	Liew et al. [30]		32.782	62.630	62.630	87.869	103.61	104.60	123.59	123.59	125.40	125.40

Table 7
Effect of knot spacing patterns on the convergence of the first ten frequency parameters Ω* for CC–CC thick square plates with $h/a = 0.4$

Spacing pattern	$(k_\xi-1)\times(k_\eta-1)\times(k_\zeta-1)$	$M_\xi\times M_\eta\times M_\zeta$	Modes									
			1st SS–A	2nd SA–A	3rd AS–A	4th SA–S^T	5th AS–S^T	6th AA–S^T	7th AA–A	8th SS–A	9th SS–A	10th AA–S^T
Uniform distribution	$3\times3\times3$	$7\times7\times9$	18.124	29.063	29.063	31.046	31.046	36.719	38.116	42.779	43.386	44.992
		$9\times9\times9$	18.109	29.046	29.046	31.035	31.035	36.717	38.096	42.724	43.323	44.970
		$11\times11\times9$	18.101	29.038	29.038	31.029	31.029	36.716	38.087	42.711	43.308	44.961
		$13\times13\times9$	18.096	29.033	29.033	31.025	31.025	36.716	38.082	42.706	43.302	44.955
		$15\times15\times9$	18.093	29.030	29.030	31.023	31.023	36.716	38.079	42.704	43.298	44.952
	$4\times4\times3$	$7\times7\times9$	18.106	29.043	29.043	31.033	31.033	36.716	38.093	42.719	43.318	44.967
		$9\times9\times9$	18.097	29.034	29.034	31.026	31.026	36.716	38.083	42.707	43.303	44.957
		$11\times11\times9$	18.093	29.030	29.030	31.023	31.023	36.716	38.078	42.703	43.298	44.952
		$13\times13\times9$	18.090	29.027	29.027	31.021	31.021	36.715	38.076	42.701	43.295	44.949
		$15\times15\times9$	18.089	29.026	29.026	31.020	31.020	36.715	38.074	42.700	43.293	44.947
Shifted Chebyshev distribution	$3\times3\times3$	$7\times7\times9$	18.098	29.065	29.065	31.028	31.028	36.730	38.123	43.014	43.627	45.011
		$9\times9\times9$	18.088	29.029	29.029	31.019	31.019	36.717	38.078	42.774	43.372	44.953
		$11\times11\times9$	18.084	29.022	29.022	31.016	31.016	36.715	38.070	42.711	43.304	44.943
		$13\times13\times9$	18.082	29.020	29.020	31.015	31.015	36.715	38.068	42.698	43.289	44.940
		$15\times15\times9$	18.081	29.019	29.019	31.014	31.014	36.715	38.067	42.695	43.286	44.939
Shifted Legendre distribution	$3\times3\times3$	$7\times7\times9$	18.095	29.084	29.084	31.026	31.026	36.741	38.150	43.111	43.725	45.043
		$9\times9\times9$	18.086	29.030	29.030	31.018	31.018	36.718	38.080	42.807	43.407	44.955
		$11\times11\times9$	18.083	29.021	29.021	31.015	31.015	36.715	38.069	42.717	43.310	44.943
		$13\times13\times9$	18.082	29.019	29.019	31.014	31.014	36.715	38.067	42.700	43.290	44.940
		$15\times15\times9$	18.081	29.019	29.019	31.014	31.014	36.715	38.066	42.695	43.286	44.939
	Zhou et al. [34]		18.085	29.020	29.020	31.015	31.015	36.715	38.067	42.694	43.285	44.940
	Liew et al. [30]		18.091	29.028	29.028	31.021	31.021	36.715	38.077	42.703	43.296	44.950

to thin, moderately thick, and thick plates, respectively. The results are compared with other published solutions by using the 3-D exact solution [8], the 3-D Ritz method with simple algebraic polynomials [27], the 3-D Ritz method with general orthogonal polynomials using the Gram-Schmidt process [30], and the 3-D Ritz method with Chebyshve polynomials [34]. The symbols * are missing frequencies [11] that were not considered by Srinivas et al. [8].

The results in Tables 8 and 9 show excellent agreement in all cases.

Tables 10 and 11 show the first ten frequency parameters Ω^* for CF–FF and FF–FF square plates ($b/a = 1$) for thickness–length ratios h/a from 0.01 to 0.5. The results are compared with other published solutions by using the 3-D Ritz method with simple algebraic polynomials [25,26,28,29], the 3-D finite element code MSC/NASTRAN [26], the 3-D Ritz method with general orthogonal polynomials [30,32], the Ritz method based on the Mindlin plate theory with $\kappa^2 = 5/6$ [42], the Ritz method based on the Reddy plate theory [46], and the exact solution based on the classical thin plate theory [43].

The results obtained by McGee and Leissa [26] in Table 10 used only few terms ($6 \times 4 \times 4$ terms) of simple algebraic polynomials, and the convergence of the results was not verified. The present results converged up to

Table 8
Comparison of the first ten frequency parameters Ω^* for SS–SS square plates

h/a	Solution methods	Modes									
		1st	2nd	3rd	4th	5th	6th	7th	8th	9th	10th
0.01		SS–A	SA–A	AS–A	AA–A	SS–A	SS–A	SA–A	AS–A	SA–A	AS–A
	Present	19.732	49.305	49.305	78.846	98.525	98.525	128.01	128.01	167.30	167.30
	Orthogonal polynomials–Ritz [30]	19.732	49.305	49.305	78.846	98.524	98.524	128.02	128.02	167.29	167.29
	Simple polynomials–Ritz [27]	19.732	49.305	49.305	78.847	98.524	98.524	128.01	128.01	167.29	167.29
0.05		SS–A	SA–A	AS–A	AA–A	SS–A	SS–A	SA–A	AS–A	SA–S^M	AS–S^M
	Present	19.569	48.311	48.311	76.361	94.700	94.700	121.70	121.70	128.77	128.77
	Simple polynomials–Ritz [27]	19.569	48.310	48.310	76.361	94.700	94.700	121.70	121.70	128.77	128.77
0.1		SS–A	SA–A	AS–A	SA–S^M	AS–S^M	AA–A	SS–A	SS–A	SS–S^M	SA–A
	Present	19.090	45.619	45.619	64.383	64.383	70.104	85.487	85.487	91.052	107.37
	Orthogonal polynomials–Ritz [30]	19.090	45.619	45.619	64.383	64.383	70.104	85.488	85.488		107.37
	Simple polynomials–Ritz [27]	19.090	45.622	45.622	64.383	64.383	70.112	85.502	85.502	91.052	107.40
	Chebyshev polynomials–Ritz [34]	19.090	45.619	45.619	64.383	64.383	70.104	85.488	85.488		
	Exact solution [8]	19.090	45.619	45.619	*	*	70.104	85.488	85.488		
0.2		SS–A	SA–S^M	AS–S^M	SA–A	AS–A	SS–S^M	AA–A	AA–S^M	AA–S^M	SS–A
	Present	17.526	32.191	32.191	38.482	38.482	45.526	55.787	64.383	64.383	65.996
	Orthogonal polynomials–Ritz [30]	17.526	32.192	32.192	38.483	38.483	45.526	55.787	64.383	64.383	65.995
	Simple polynomials–Ritz [27]	17.528	32.192	32.192	38.502	38.502	45.526	55.843	64.383	64.383	66.086
	Chebyshev polynomials–Ritz [34]	17.526	32.192	32.192	38.483	38.483	45.527	55.787	64.383		
	Exact solution [8]	17.525	*	*	38.483	38.483	45.527	55.790	*	*	
0.3		SS–A	SA–S^M	AS–S^M	SS–S^M	SA–A	AS–A	AA–S^M	AA–S^M	AA–A	SA–S^M
	Present	15.688	21.461	21.461	30.351	31.983	31.983	42.922	42.922	44.534	47.988
	Orthogonal polynomials–Ritz [30]	15.688	21.461	21.461	30.351	31.983	31.983	42.922	42.922	44.535	47.989
0.4		SS–A	SA–S^M	AS–S^M	SS–S^M	SA–A	AS–A	AA–S^M	AA–S^M	SA–S^M	AS–S^M
	Present	13.947	16.096	16.096	22.763	26.898	26.898	32.191	32.191	35.991	35.991
	Orthogonal polynomials–Ritz [30]	13.947	16.096	16.096	22.763	26.899	26.899	32.192	32.192	35.991	35.991
0.5		SS–A	SA–S^M	AS–S^M	SS–S^M	SA–A	AS–A	AA–S^M	AA–S^M	SA–A^M	AS–A^M
	Present	12.426	12.877	12.877	18.210	23.007	23.007	25.753	25.753	28.793	28.793
	Orthogonal polynomials–Ritz [30]	12.426	12.877	12.877	18.210	23.008	23.008	25.754	25.754	28.794	28.794
	Chebyshev polynomials–Ritz [34]	12.426	12.877	12.877	18.210	23.008	23.008	25.754	25.754		
	Exact solution [8]	12.426	*	*	18.210			*	*	*	*

*are missing frequencies [11].

Table 9
Comparison of the first ten frequency parameters Ω^* for CC–CC square plates

h/a	Solution methods	Modes									
		1st	2nd	3rd	4th	5th	6th	7th	8th	9th	10th
0.01		SS–A	SA–A	AS–A	AA–A	SS–A	SS–A	SA–A	AS–A	SA–A	AS–A
	Present	35.977	73.315	73.315	108.00	131.39	132.02	164.56	164.56	211.26	211.26
	Orthogonal polynomials–Ritz [30]	36.016	73.382	73.382	108.10	131.41	132.05	164.64	164.64	209.89	209.89
	Simple polynomials–Ritz [27]	36.097	73.521	73.521	108.30	131.70	132.34	165.00	165.00	210.27	210.27
0.05		SS–A	SA–A	AS–A	AA–A	SS–A	SS–A	SA–A	AS–A	SA–A	AS–A
	Present	35.094	70.138	70.138	101.58	122.31	123.08	151.08	151.08	189.69	189.69
	Simple polynomials–Ritz [27]	35.163	70.259	70.259	101.74	122.52	123.30	151.33	151.33	189.91	189.91
0.1		SS–A	SA–A	AS–A	AA–A	SS–A	SS–A	SA–S^{T}	AS–S^{T}	SA–A	AS–A
	Present	32.749	62.577	62.577	87.801	103.60	104.59	123.55	123.55	125.36	125.36
	Orthogonal polynomials–Ritz [30]	32.782	62.630	62.630	87.869	103.61	104.60	123.59	123.59	125.40	125.40
	Simple polynomials–Ritz [27]	32.797	62.672	62.672	87.941	103.71	104.70	123.60	123.60	125.53	125.53
	Chebyshev polynomials–Ritz [34]	32.743	62.562	62.562	87.783	103.51	104.49	123.55	123.55	125.29	125.29
0.2		SS–A	SA–A	AS–A	SA–S^{T}	AS–S^{T}	AA–A	SS–A	SS–A	AA–S	SA–A
	Present	26.889	47.080	47.080	61.906	61.906	63.322	72.274	73.267	73.400	85.829
	Orthogonal polynomials–Ritz [30]	26.906	47.103	47.103	61.917	61.917	63.348	72.286	73.281	73.400	85.846
	Simple polynomials–Ritz [27]	26.974	47.253	47.253	61.944	61.944	63.570	72.568	73.403	73.580	86.210
	Chebyshev polynomials–Ritz [34]	26.886	47.074	47.074	61.904	61.904	63.315	72.253	73.243	73.399	85.810
0.3		SS–A	SA–A	AS–A	SA–S^{T}	AS–S^{T}	AA–A	AA–S^{T}	SS–A	SS–A	AA–S^{T}
	Present	21.859	36.218	36.218	41.326	41.326	47.849	48.944	53.889	54.669	60.056
	Orthogonal polynomials–Ritz [30]	21.869	36.228	36.228	41.333	41.333	47.861	48.944	53.893	54.676	60.066
	Chebyshev polynomials–Ritz [34]	21.857	36.215	36.215	41.325	41.325	47.846	48.944	53.879	54.658	60.054
0.4		SS–A	SA–A	AS–A	SA–S^{T}	AS–S^{T}	AA–S^{T}	AA–A	SS–A	SS–A	AA–S^{T}
	Present	18.082	29.020	29.020	31.015	31.015	36.715	38.067	42.699	43.290	44.940
	Orthogonal polynomials–Ritz [30]	18.091	29.028	29.028	31.021	31.021	36.715	38.077	42.703	43.296	44.950
	Chebyshev polynomials–Ritz [34]	18.085	29.020	29.020	31.015	31.015	36.715	38.067	42.694	43.285	44.940
0.5		SS–A	SA–A	AS–A	SA–S^{T}	AS–S^{T}	AA–S^{T}	AA–A	SS–A	SS–A	AA–S^{T}
	Present	15.286	24.071	24.071	24.816	24.816	29.376	31.502	35.304	35.756	35.802
	Orthogonal polynomials–Ritz [30]	15.294	24.078	24.078	24.823	24.823	29.377	31.510	35.308	35.763	35.812
	Chebyshev polynomials–Ritz [34]	15.286	24.071	24.071	24.817	24.817	29.376	31.502	35.302	35.754	35.802

at least four significant digits and show an excellent upper bound behavior compared to other results (see, Refs. [26,29]). From Table 11, good accuracy was also obtained for all thickness–length ratios h/a.

In the Ritz method, when the essential boundary condition of the plate such as the displacement amplitude components are satisfied, the natural boundary condition of the plate such as six stress components are also automatically satisfied. However, the accuracy of the stress mode shapes must be established, and this has not been reported so far. To achieve this it is necessary (1) to examine accuracy of stress modes, and (2) to check stress free boundary conditions at the top and bottom surfaces. Table 12 gives the accuracy of the displacement amplitude and stress modes for SS–SS isotropic square plates ($b/a = 1$) for thickness–length ratio $h/a = 0.3$. The results are compared with those obtained by Srinivas et al. [8] using the exact solution.

It is seen that high accuracy are obtained for both the displacement amplitudes and each of the stress modes. Table 12 also shows that the natural boundary conditions are also approximately satisfied.

These solutions have so far only been obtained for plates with four simple supported edges by solving a set of simultaneous partial differential equations as the governing equation [8–10]. Other boundary conditions such as clamped and stress free edges are very difficult to solve with this set of simultaneous partial differential equations by either exact or analytical solutions. The proposed method however yields highly accurate results for natural frequencies, amplitude displacements and stress modes of the isotropic plate. In addition, stable

Table 10
Comparison of the first ten frequency parameters Ω^* for CF–FF square plates

h/a	Solution methods	Modes									
		1st	2nd	3rd	4th	5th	6th	7th	8th	9th	10th
0.01		S–A	A–A^T	S–A	S–A	A–A^T	S–A	S–A	A–A^T	A–A^T	A–A^T
	Present	3.4712	8.4826	21.273	27.150	30.861	53.951	61.278	64.078	70.862	92.586
	Simple polynomials–Ritz [29]	3.4895	8.5353	21.375	27.214	31.064	54.413	61.458	64.201	71.342	94.930
0.05		S–A	A–A^T	S–A	S–A	A–A^T	A–S ^{T}	S–A	S–A	A–A^T	A–A^T
	Present	3.4627	8.3382	20.969	26.653	30.043	43.549	51.858	59.264	61.969	68.005
	Simple polynomials–Ritz [29]	3.4757	8.3850	21.054	26.721	30.230	43.704	52.305	59.486	62.154	68.495
0.1		S–A	A–A^T	S–A	A–S^T	S–A	A–A^T	S–A	S–S	S–A	A–A^T
	Present	3.4387	8.0746	20.152	21.796	25.541	28.325	47.677	52.302	54.400	57.190
	Simple polynomials–Ritz [29]	3.4480	8.0996	20.209	21.864	25.574	28.438	47.921	52.366	54.550	57.301
0.2		S–A	A–A^T	A–S^T	S–A	S–A	A–A^T	S–S	A–S^T	S–A	S–A
	Present	3.3545	7.3743	10.918	17.697	22.557	24.034	26.195	29.283	38.590	43.091
	Simple polynomials–Ritz [26]	3.3687	7.3397	10.985	17.695	23.689	25.000	26.234	29.388		
	FEM [26]	3.3624	7.3941	10.944	17.673	22.149	23.950	26.228	29.187		
	Simple polynomials–Ritz [29]	3.3618	7.3880	10.950	17.736	22.574	24.093	26.223	29.304	38.697	43.207
0.3		S–A	A–A^T	A–S^T	S–A	S–S	A–S^T	S–A	A–A^T	S–S	S–A
	Present	3.2336	6.5976	7.2902	15.077	17.488	19.520	19.591	20.107	30.948	31.390
0.4		S–A	A–S^T	A–A^T	S–A	S–S	A–S^T	A–A^T	S–A	S–S	A–S^T
	Present	3.0889	5.4756	5.8553	12.794	13.131	14.638	17.000	17.073	23.165	25.120
0.5		S–A	A–S^T	A–A^T	S–S	S–A	A–S^T	A–A^T	S–A	S–S	A–S^T
	Present	2.9331	4.3865	5.1925	10.516	10.937	11.708	14.599	15.024	18.478	20.096
	Simple polynomials–Ritz [25]	2.9564	4.4112	5.2100	10.549	10.999	11.727	14.670	15.054	18.488	20.277
	Simple polynomials–Ritz [26]	2.9463	4.4178	5.1815	10.539	10.979	11.754	14.467	16.166		
	FEM [26]	2.9397	4.3957	5.1470	10.520	10.786	11.663	14.327	14.479		
	Orthogonal polynomials–Ritz [30]	2.9372	4.3910	5.1944	10.548	10.942	11.708	14.602	15.024	18.478	20.103
	Simple polynomials–Ritz [28]	2.9353	4.3948	5.1938	10.522	10.939	11.712	14.602	15.024	18.478	20.115

and rapidly converging as well as excellent upper bound solutions are obtained by the proposed method regardless of the thickness–length ratios h/a and boundary conditions, and numerical stability is also observed.

4.3. Parametric studies

The last section, the present method is applied to investigate the free vibration of CF–FF rectangular plates. Table 13 gives the effects of the thickness–length ratios h/a and the aspect ratios b/a on the first 12 frequency parameters Ω^* for cantilevered isotropic rectangular plates for h/a from 0.01 to 0.5, and, $b/a = 0.5$, 1, 1.5, and 2. To obtain accurate results, this sub-section used the following parameters: the degree of spline functions are set as $(k_\xi-1)\times(k_\eta-1)\times(k_\zeta-1) = 4\times4\times2$ for $h/a\leqslant0.05$, and $k_\xi-1\times k_\eta-1\times k_\zeta-1 = 4\times4\times3$ for $h/a\geqslant0.1$; the number of knots $M_\xi\times M_\eta\times M_\zeta = 21\times21\times5$ for $h/a\leqslant0.05$, $M_\xi\times M_\eta\times M_\zeta = 15\times15\times7$ for $0.1\leqslant h/a\leqslant0.3$, and $M_\xi\times M_\eta\times M_\zeta = 15\times15\times9$ for $h/a>0.3$; and the shifted Chebyshev distribution knot spacing pattern is used here. Note that the symmetric modes in the ζ direction (U and V are symmetric distributions in the ζ direction, and W is anti-symmetric distribution in the ζ direction) cannot be expressed by the approximate theories for moderately thick plate without in-plane displacement components.

It is seen when the thickness–length ratio h/a increases, the frequency parameters decrease regardless of the aspect ratio b/a, and when the aspect ratio b/a increases, the frequency parameters increase. It seems that the effects of stress–strain in the thickness direction, transverse shear deformation, and rotational inertia appear. As a result, symmetric modes in the ζ direction easily appear in low-order vibrations. Moreover, well known, thickness modes also appear in low-order vibrations for CC–CC plates (Table 9). Therefore, the formulation

Table 11
Comparison of the first ten frequency parameters Ω^* for FF–FF square plates

h/a	Solution method	Modes									
		1st	2nd	3rd	4th	5th	6th	7th	8th	9th	10th
0.01		AA–A	SS–A	SS–A	SA–A	AS–A	SA–A	AS–A	SS–A	AA–A	AA–A
	Present	13.419	19.589	24.258	34.669	34.669	61.016	61.016	63.355	68.984	76.932
	CPT-exact [43]	13.489	19.789	24.432	35.024	35.024	61.526	61.526			
		AA–A	SS–A	SS–A	SA–A	AS–A	SA–A	AS–A	SS–A	AA–A	AA–A
0.05	Present	13.147	19.425	24.018	33.727	33.727	59.477	59.477	60.739	66.299	74.104
0.1		AA–A	SS–A	SS–A	SA–A	AS–A	SA–A	AS–A	SS–A	AA–A	AA–A
	Present	12.723	18.954	23.345	31.955	31.955	55.490	55.490	55.821	60.760	67.875
	3-D Ritz [32]	12.726	18.955	23.347	31.965	31.965	55.493	55.493	55.853	60.767	67.882
	Reddy–Ritz [46]	12.722	18.944	23.325	31.931	31.931	55.741	55.358	55.358	60.655	67.694
	Mindlin–Ritz [42]	12.719	18.945	23.323	31.922	31.922	55.351	55.351	55.715	60.632	67.674
0.2		AA–A	SS–A	SS–A	SA–A	AS–A	AA–S^M	SA–S^T	AS–S^T	SS–A	SS–S^M
	Present	11.710	17.433	21.252	27.647	27.647	40.192	42.775	42.775	45.308	45.526
	3-D Ritz [32]	11.710	17.433	21.252	27.647	27.647	40.191	42.776	42.776	45.310	
	Mindlin–Ritz [42]	11.701	17.400	21.194	27.573	27.573	*	*	*	45.105	*
0.3		AA–A	SS–A	SS–A	SA–A	AS–A	AA–S^M	SA–S^T	AS–S^T	SS–S^M	SS–S^T
	Present	10.648	15.657	18.914	23.613	23.613	26.793	28.488	28.488	30.351	34.376
0.4		AA–A	SS–A	SS–A	AA–S^M	SA–A	AS–A	SA–S^T	AS–S^T	SS–S^M	SS–S^T
	Present	9.6577	13.980	16.781	20.093	20.297	20.297	21.333	21.333	22.763	25.697
0.5		AA–A	SS–A	SS–A	AA–S^M	SA–S^T	AS–S^T	SA–A	AS–A	SS–S^M	SS–S^T
	Present	8.7800	12.515	14.961	16.072	17.030	17.030	17.631	17.631	18.210	20.451
	3-D Ritz [32]	8.7802	12.515	14.962	16.073	17.030	17.030	17.631	17.631	18.211	

Notes that first six rigid modes are cut off.
*Denotes symmetric modes in the ζ direction, which cannot be expressed by Mindlin and Reddy plate theory.

of numerical method should be based on the theory of elasticity to analyze 3-D free vibration of isotropic rectangular plates having any stress free edges.

5. Conclusions

This paper proposed the B-spline Ritz method based on the linear and small strain theory of elasticity, and the Ritz procedure to analyze 3-D free vibration of isotropic rectangular plates with any thicknesses and arbitrary boundary conditions. A triplicate series of B-spline functions is chosen as the trial functions of the amplitude displacement functions. With the proposed method, the knot spacing pattern can be arranged freely across an analysis domain. In addition, the method can analyze by using lower degree of the polynomials than the Ritz method with global functions. The proposed method may be considered to be the piecewise Ritz method and is applicable to very thin as well as to thick rectangular plates. Stable numerical computation, rapid convergence, and high accuracy are observed in the analysis. Especially, more accurate results are obtained by using both the low-order degree of spline functions and the non-uniform knot spacing pattern. The frequency parameters and vibration modes of cantilevered rectangular plates of different thickness–length and aspect ratios are also investigated in detail. The present results may serve as benchmark data for validating 3-D finite element solutions, and future developments in new numerical methods.

The B-spline Ritz method has been shown to be simple, powerful, efficient, and effective in analyzing 3-D free vibrations of isotropic rectangular plates with arbitrary thickness and/or boundary conditions. In further research, it would be possible to consider the potential of the proposed method in 3-D free vibration analysis of other structural elements with different geometric shapes and materials.

Table 12
Comparison of the displacement amplitude and stress modes for SS–SS square plate

Modes	ζ	$U/U_{\max}$		$V/V_{\max}$		$W/W_{\max}$		$\sigma_x/\sigma_{x\ \max} = \sigma_y/\sigma_{y\ \max}$		$\sigma_z/\sigma_{z\ \max}$		$\tau_{xy}/\tau_{xy\ \max}$		$\tau_{yz}/\tau_{yz\ \max} = \tau_{zx}/\tau_{zx\ \max}$	
		Present	Exact [8]	Present	Exact [8]	Present	Exact [8]	Present	Exact [8]	Present	Exact [8]	Present	Exact [8]	Present	Exact [8]
1st mode	0	1.0000	1	1.0000	1	0.9406	0.9406	1.0000	1	0.0004	0	1.0000	1	0.0000	0
SS–A	0.1	0.7561	0.7561	0.7561	0.7561	0.9641	0.9641	0.7676	0.7676	0.7579	0.7578	0.7561	0.7561	0.3750	0.3750
	0.2	0.5420	0.5420	0.5420	0.5420	0.9807	0.9807	0.5571	0.5571	1.0000	1	0.5420	0.5420	0.6549	0.6549
	0.3	0.3496	0.3496	0.3496	0.3496	0.9917	0.9917	0.3627	0.3627	0.8685	0.8686	0.3496	0.3496	0.8487	0.8426
	0.4	0.1713	0.1713	0.1713	0.1713	0.9980	0.9980	0.1788	0.1787	0.4941	0.4941	0.1713	0.1713	0.9625	0.9625
	0.5	0.0000	0	0.0000	0	1.0000	1	0.0000	0	0.0000	0	0.0000	0	1.0000	1
	0.6	−0.1713		−0.1713		0.9980		−0.1788		−0.4941		−0.1713		0.9625	
	0.7	−0.3496		−0.3496		0.9917		−0.3627		−0.8685		−0.3496		0.8487	
	0.8	−0.5420		−0.5420		0.9807		−0.5571		−1.0000		−0.5420		0.6549	
	0.9	−0.7561		−0.7561		0.9641		−0.7676		−0.7579		−0.7561		0.3750	
	1	−1.0000		−1.0000		0.9406		−1.0000		−0.0004		−1.0000		0.0000	
42th mode	0	1.0000	1	1.0000	1	1.0000	1	1.0000	1	0.0001	0	1.0000	1	0.0000	0
SS–A	0.1	0.9892	0.9892	0.9892	0.9892	0.8149	0.8148	0.9174	0.9174	0.7064	0.7063	0.9892	0.9892	0.2926	0.2925
	0.2	0.8655	0.8655	0.8655	0.8655	0.6166	0.6166	0.7638	0.7638	1.0000	1	0.8655	0.8655	0.5703	0.5703
	0.3	0.6409	0.6409	0.6409	0.6409	0.4426	0.4426	0.5481	0.5481	0.9129	0.9129	0.6409	0.6409	0.7984	0.7984
	0.4	0.3407	0.3407	0.3407	0.3407	0.3244	0.3243	0.2863	0.2863	0.5350	0.5350	0.3407	0.3407	0.9479	0.9479
	0.5	0.0000	0	0.0000	0	0.2825	0.2825	0.0000	0	0.0000	0	0.0000	0	1.0000	1
	0.6	−0.3407		−0.3407		0.3244		−0.2863		−0.5350		−0.3407		0.9479	
	0.7	−0.6409		−0.6409		0.4426		−0.5481		−0.9129		−0.6409		0.7984	
	0.8	−0.8655		−0.8655		0.6166		−0.7638		−1.0000		−0.8655		0.5703	
	0.9	−0.9892		−0.9892		0.8149		−0.9174		−0.7064		−0.9892		0.2926	
	1	−1.0000		−1.0000		1.0000		−1.0000		0.0001		−1.0000		0.0000	
12th mode	0	0.8861	0.8861	0.8861	0.8861	1.0000	1	0.9537	0.9537	0.0001	0	0.8861	0.8861	0.0002	0
SS–S^T	0.1	0.9248	0.9249	0.9248	0.9249	0.8280	0.8280	0.9690	0.9690	0.3458	0.3458	0.9248	0.9249	0.7426	0.7425
	0.2	0.9567	0.9567	0.9567	0.9567	0.6377	0.6377	0.9820	0.9820	0.6257	0.6257	0.9567	0.9567	1.0000	1
	0.3	0.9804	0.9804	0.9804	0.9804	0.4333	0.4333	0.9918	0.9918	0.8316	0.8316	0.9804	0.9804	0.8813	0.8813
	0.4	0.9951	0.9950	0.9951	0.9950	0.2191	0.2191	0.9979	0.9979	0.9576	0.9576	0.9951	0.9950	0.5057	0.5057
	0.5	1.0000	1	1.0000	1	0.0000	0	1.0000	1	1.0000	1	1.0000	1	0.0000	0
	0.6	0.9951		0.9951		−0.2191		0.9979		0.9576		0.9951		−0.5057	
	0.7	0.9804		0.9804		−0.4333		0.9918		0.8316		0.9804		−0.8813	
	0.8	0.9567		0.9567		−0.6377		0.9820		0.6257		0.9567		−1.0000	
	0.9	0.9248		0.9248		−0.8280		0.9690		0.3458		0.9248		−0.7426	
	1	0.8861		0.8861		−1.0000		0.9537		0.0001		0.8861		−0.0002	

Table 13
Results at various thickness–length ratios h/a and the aspect ratios b/a for the first twelve frequency parameters $\Omega*$ of CF–FF rectangular plates

b/a	h/a	Modes											
		1st	2nd	3rd	4th	5th	6th	7th	8th	9th	10th	11th	12th
0.5	0.01	S–A	A–A^t	S–A	A–A^t	S–A	A–A^t	S–A	S–A	S–A	A–S^t	A–A^t	S–A
		0.85969	3.6781	5.3553	11.970	15.019	22.987	23.214	29.556	31.547	35.913	37.984	44.332
	0.05	S–A	A–A^t	S–A	A–S^t	A–A^t	S–A	A–A^t	S–A	S–S	A–S^t	S–A	S–A
		0.85658	3.5494	5.2800	7.1914	11.449	14.535	21.653	22.300	26.091	27.401	27.820	29.541
	0.1	S–A	A–A^t	A–S^t	S–A	A–A^t	S–S	S–A	A–S^t	A–A^t	S–A	S–A	S–A
		0.84971	3.3229	3.6007	5.0732	10.480	13.057	13.343	13.704	19.117	20.229	24.234	25.743
	0.2	S–A	A–S^t	A–A^t	S–A	S–S	A–S^t	A–A^t	S–A	A–S^t	A–A^t	S–A	S–A
		0.82862	1.8048	2.7804	4.4496	6.5388	6.8544	8.4026	10.579	14.345	14.370	15.861	17.667
	0.3	S–A	A–S^t	A–A^t	S–A	S–S	A–S^t	A–A^t	S–A	A–S^t	A–A^t	A–S^t	S–A
		0.79944	1.2059	2.2603	3.7861	4.3648	4.5709	6.7245	8.4038	9.5582	11.123	12.240	12.541
	0.4	S–A	A–S^t	A–A^t	S–A	S–S	A–S^t	A–A^t	S–A	A–S^t	A–A^t	A–S^t	S–S
		0.76456	0.90644	1.8286	3.2110	3.2769	3.4291	5.4548	6.8584	7.1626	8.9066	9.1787	9.4583
	0.5	A–S^t	S–A	A–A^t	S–S	A–S^t	S–A	A–A^t	A–S^t	S–A	A–A^t	A–S^t	S–A
		0.72670	0.72672	1.4899	2.6237	2.7439	2.7440	4.4612	5.7202	5.7203	6.8916	7.3406	7.3406
1	0.01	S–A	A–A^t	S–A	S–A	A–A^t	S–A	S–A	A–A^t	A–A^t	A–A^t	S–A	S–A
		3.4712	8.4822	21.270	27.147	30.857	53.940	61.197	64.008	70.778	92.498	96.594	118.95
	0.05	S–A	A–A^t	S–A	S–A	A–A^t	A–S^t	S–A	S–A	A–A^t	A–A^t	A–A^t	S–A
		3.4626	8.3379	20.968	26.652	30.041	43.548	51.855	59.257	61.964	67.998	87.820	91.262
	0.1	S–A	A–A^t	S–A	A–S^t	S–A	A–A^t	S–A	S–S	S–A	A–A^t	A–S^t	A–A^t
		3.4386	8.0742	20.151	21.796	25.540	28.324	47.674	52.302	54.393	57.186	58.567	61.829
	0.2	S–A	A–A^t	A–S^t	S–A	S–A	A–A^t	S–S	A–S^t	S–A	S–A	A–A^t	S–S
		3.3543	7.3737	10.917	17.695	22.556	24.031	26.194	29.283	38.585	43.083	45.747	46.482
	0.3	S–A	A–A^t	A–S^t	S–A	S–S	A–S^t	S–A	A–A^t	S–S	S–A	A–S^t	S–A
		3.2332	6.5967	7.2900	15.074	17.488	19.520	19.589	20.104	30.948	31.385	33.489	34.214
	0.4	S–A	A–S^t	A–A^t	S–A	S–S	A–S^t	A–A^t	S–A	S–S	A–S^t	S–A	S–S
		3.0887	5.4756	5.8550	12.793	13.131	14.638	16.999	17.073	23.165	25.120	26.134	26.501
	0.5	S–A	A–S^t	A–A^t	S–S	S–A	A–S^t	A–A^t	S–A	S–S	A–S^t	S–S	S–A
		2.9329	4.3865	5.1921	10.516	10.936	11.708	14.598	15.024	18.478	20.096	21.112	22.238

Table 13 (*continued*)

b/a	h/a	Modes											
		1st	2nd	3rd	4th	5th	6th	7th	8th	9th	10th	11th	12th
1.5	0.01	S–A	A–A^t	S–A	S–A	A–A^t	A–A^t	S–A	A–A^t	S–A	S–A	A–A^t	S–A
		7.8424	14.345	32.480	49.292	58.175	70.687	86.069	127.05	127.13	138.48	147.07	175.28
	0.05	S–A	A–A^t	S–A	S–A	A–A^t	A–A^t	S–A	A–S^t	A–A^t	S–A	S–A	A–A^t
		7.8264	14.174	31.983	48.633	56.951	69.348	83.526	113.62	122.37	123.21	134.13	141.80
	0.1	S–A	A–A^t	S–A	S–A	A–A^t	A–S^t	A–A^t	S–A	A–A^t	S–A	S–S	S–A
		7.7765	13.858	30.982	46.737	54.183	56.851	66.269	78.165	112.55	114.87	117.34	123.29
	0.2	S–A	A–A^t	S–A	A–S^t	S–A	A–A^t	A–A^t	S–S	A–S^t	S–A	S–S	S–S
		7.5916	12.985	28.267	28.462	40.951	46.731	57.916	58.765	64.257	65.343	74.424	88.977
	0.3	S–A	A–A^t	A–S^t	S–A	S–A	S–S	A–A^t	A–S^t	S–S	A–A^t	S–A	S–S
		7.3188	11.957	18.997	25.348	34.806	39.233	39.415	42.849	49.588	49.627	54.230	59.285
	0.4	S–A	A–A^t	A–S^t	S–A	S–S	S–A	A–S^t	A–A^t	S–S	A–A^t	S–S	S–A
		6.9902	10.920	14.263	22.667	29.461	29.514	32.141	33.342	37.156	42.543	44.420	45.736
	0.5	S–A	A–A^t	A–S^t	S–A	S–S	S–A	A–S^t	A–Ai^t	S–S	S–S	A–A^t	S–A
		6.6350	9.9520	11.421	20.333	23.594	25.255	25.714	28.486	29.685	35.484	36.597	39.306
2	0.01	S–A	A–A^t	S–A	A–A^t	S–A	A–A^t	S–A	S–A	A–A^t	A–A^t	S–A	S–A
		13.974	21.373	40.646	76.237	87.325	98.564	125.50	136.60	171.89	214.91	232.18	245.54
	0.05	S–A	A–A^t	S–A	A–A^t	S–A	A–A^t	S–A	S–A	A–A^t	A–A^t	A–S^t	S–A
		13.948	21.174	40.100	74.987	86.159	96.823	122.35	133.32	166.54	205.39	216.29	223.13
	0.1	S–A	A–A^t	S–A	A–A^t	S–A	A–A^t	A–S^t	S–A	S–A	A–A^t	A–A^t	S–S
		13.863	20.801	39.037	72.433	82.798	92.523	108.21	115.67	127.07	155.29	192.55	201.19
	0.2	S–A	A–A^t	S–A	A–S^t	A–A^t	S–A	A–A^t	S–A	S–S	S–A	A–S^t	S–S
		13.540	19.741	36.111	54.155	65.306	72.530	80.396	98.524	100.70	110.29	111.48	111.84
	0.3	S–A	A–A^t	S–A	A–S^t	A–A^t	S–A	S–S	A–A^t	A–S^t	S–S	S–A	S–S
		13.057	18.444	32.844	36.135	57.615	61.601	67.193	68.240	74.365	74.598	82.584	90.049
	0.4	S–A	A–A^t	A–S^t	S–A	S–S	A–A^t	S–A	A–S^t	S–S	A–A^t	S–S	S–A
		12.471	17.085	27.123	29.740	50.431	50.508	52.166	55.799	55.957	58.172	67.512	69.854
	0.5	S–A	A–A^t	A–S^t	S–A	S–S	A–A^t	S–A	A–S^t	S–S	A–A^t	S–S	S–A
		11.836	15.776	21.714	26.982	40.368	44.222	44.540	44.654	44.758	50.282	53.977	59.917

Acknowledgments

Financial support from the Japan Society for the Promotion of Science (JSPS) is gratefully acknowledged.

Appendix A

The sub-stiffness and mass matrices in Eq. (33) are given as follows:

$$
\begin{aligned}
[K_{UU}] &= \sum\left[\overline{\Delta}_1 I_{mi}^{11} J_{nj}^{00} P_{rs}^{00} + \overline{\Delta}_3\left\{\left(\frac{a}{b}\right)^2 I_{mi}^{00} J_{nj}^{11} P_{rs}^{00} + \left(\frac{a}{h}\right)^2 I_{mi}^{00} J_{nj}^{00} P_{rs}^{11}\right\}\right],\\
[K_{UV}] &= \sum\left\{\overline{\Delta}_2\left(\frac{a}{b}\right) I_{mi}^{10} J_{nj}^{01} P_{rs}^{00} + \overline{\Delta}_3\left(\frac{a}{b}\right) I_{mi}^{01} J_{nj}^{10} P_{rs}^{00}\right\},\\
[K_{UW}] &= \sum\left\{\overline{\Delta}_2\left(\frac{a}{h}\right) I_{mi}^{10} J_{nj}^{00} P_{rs}^{01} + \overline{\Delta}_3\left(\frac{a}{h}\right) I_{mi}^{01} J_{nj}^{00} P_{rs}^{10}\right\},\\
[K_{VU}] &= \sum\left\{\overline{\Delta}_2\left(\frac{a}{b}\right) I_{mi}^{01} J_{nj}^{10} P_{rs}^{00} + \overline{\Delta}_3\left(\frac{a}{b}\right) I_{mi}^{10} J_{nj}^{01} P_{rs}^{00}\right\},\\
[K_{VV}] &= \sum\left[\overline{\Delta}_1\left(\frac{a}{b}\right)^2 I_{mi}^{00} J_{nj}^{11} P_{rs}^{00} + \overline{\Delta}_3\left\{I_{mi}^{11} J_{nj}^{00} P_{rs}^{00} + \left(\frac{a}{h}\right)^2 I_{mi}^{00} J_{nj}^{00} P_{rs}^{11}\right\}\right],\\
[K_{VW}] &= \sum\left\{\overline{\Delta}_2\left(\frac{a}{b}\right)\left(\frac{a}{h}\right) I_{mi}^{00} J_{nj}^{10} P_{rs}^{01} + \overline{\Delta}_3\left(\frac{a}{b}\right)\left(\frac{a}{h}\right) I_{mi}^{00} J_{nj}^{01} P_{rs}^{10}\right\},\\
[K_{WU}] &= \sum\left\{\overline{\Delta}_2\left(\frac{a}{h}\right) I_{mi}^{01} J_{nj}^{00} P_{rs}^{10} + \overline{\Delta}_3\left(\frac{a}{h}\right) I_{mi}^{10} J_{nj}^{00} P_{rs}^{01}\right\},\\
[K_{WV}] &= \sum\left\{\overline{\Delta}_2\left(\frac{a}{b}\right)\left(\frac{a}{h}\right) I_{mi}^{00} J_{nj}^{01} P_{rs}^{10} + \overline{\Delta}_3\left(\frac{a}{b}\right)\left(\frac{a}{h}\right) I_{mi}^{00} J_{nj}^{10} P_{rs}^{01}\right\},\\
[K_{WW}] &= \sum\left[\overline{\Delta}_1\left(\frac{a}{h}\right)^2 I_{mi}^{00} J_{nj}^{00} P_{rs}^{11} + \overline{\Delta}_3\left\{\left(\frac{a}{b}\right)^2 I_{mi}^{00} J_{nj}^{11} P_{rs}^{00} + I_{mi}^{11} J_{nj}^{00} P_{rs}^{00}\right\}\right],\\
[K_{UU}^L] &= k_\alpha\left\{\sum(I_{mi} J_{nj}^{00} P_{rs}^{00})\Big|_{\xi=0,1} + \left(\frac{a}{b}\right)\sum(I_{mi}^{00} J_{nj} P_{rs}^{00})\Big|_{\eta=0,1}\right\},\\
[K_{VV}^L] &= k_\beta\left\{\sum(I_{mi} J_{nj}^{00} P_{rs}^{00})\Big|_{\xi=0,1} + \left(\frac{a}{b}\right)\sum(I_{mi}^{00} J_{nj} P_{rs}^{00})\Big|_{\eta=0,1}\right\},\\
[K_{WW}^L] &= k_\gamma\left\{\sum(I_{mi} J_{nj}^{00} P_{rs}^{00})\Big|_{\xi=0,1} + \left(\frac{a}{b}\right)\sum(I_{mi}^{00} J_{nj} P_{rs}^{00})\Big|_{\eta=0,1}\right\},
\end{aligned}
$$

and

$$
\begin{aligned}
[M_{UU}] &= \sum(I_{mi}^{00} J_{nj}^{00} P_{rs}^{00}), \quad [M_{VV}] = \sum(I_{mi}^{00} J_{nj}^{00} P_{rs}^{00}),\\
[M_{WW}] &= \sum(I_{mi}^{00} J_{nj}^{00} P_{rs}^{00}),
\end{aligned}
$$

where $\sum = \sum_{m=1}^{i_\xi}\sum_{n=1}^{i_\eta}\sum_{r=1}^{i_\zeta}\sum_{i=1}^{i_\xi}\sum_{j=1}^{i_\eta}\sum_{s=1}^{i_\zeta}$, the non-dimensional spring parameters k_α, k_β, and k_γ, the values of B-spline functions I_{mi} and J_{nj}, and the integrals I_{mi}^{tu}, J_{nj}^{tu}, and P_{rs}^{tu} are defined by

$$
\begin{aligned}
&k_\alpha = \frac{\alpha a}{E}, \quad k_\beta = \frac{\beta a}{E}, \quad k_\gamma = \frac{\gamma a}{E}, \quad I_{mi} = N_{m,k}(\xi) N_{i,k}(\xi), \quad J_{nj} = N_{n,k}(\eta) N_{j,k}(\eta),\\
&I_{mi}^{tu} = \int_0^1 \frac{\mathrm{d}^t N_{m,k}(\xi)}{\mathrm{d}\xi^t}\frac{\mathrm{d}^u N_{i,k}(\xi)}{\mathrm{d}\xi^u}\,\mathrm{d}\xi, \quad J_{nj}^{tu} = \int_0^1 \frac{\mathrm{d}^t N_{n,k}(\eta)}{\mathrm{d}\eta^t}\frac{\mathrm{d}^u N_{j,k}(\eta)}{\mathrm{d}\eta^u}\,\mathrm{d}\eta,\\
&P_{rs}^{tu} = \int_0^1 \frac{\mathrm{d}^t N_{r,k}(\zeta)}{\mathrm{d}\zeta^t}\frac{\mathrm{d}^u N_{s,k}(\zeta)}{\mathrm{d}\zeta^u}\,\mathrm{d}\zeta,
\end{aligned}
$$

in which t and u are the order of derivatives of the 1-D normalized B-spline functions. Those integrations are performed by using the Gauss–Legendre quadrature with k_l ($l = \xi$, η, and ζ) points.

References

[1] R.D. Mindlin, Influence of rotatory inertia and shear on flexural motions of isotropic, elastic plates, *ASEM Journal of Applied Mechanics* 73 (1951) 31–38.

[2] M. Levinson, An accurate simple theory of the static and dynamics of elastic plates, *Mechanics Research Communications* 7 (1980) 343–350.

[3] J.N. Reddy, A simple high-order theory for laminated composite plates, *ASEM Journal of Applied Mechanics* 45 (1984) 745–752.

[4] J.N. Reddy, N.D. Phan, Stability and vibration of isotropic, orthotropic and laminated plates according to a high-order shear deformation theory, *Journal of Sound and Vibration* 98 (1985) 157–170.

[5] F.N. Hanna, A.W. Leissa, A higher order shear deformation theory for the vibration of thick plates, *Journal of Sound and Vibration* 170 (1994) 545–555.

[6] H. Matsunaga, Vibration and stability of thick plates on elastic foundations, *ASCE Journal of Engineering Mechanics* 126 (1997) 27–34.

[7] R.C. Battra, S. Aimmanee, Vibrations of thick plates with higher order shear and normal deformable plate theories, *Computers and Structures* 83 (2005) 934–955.

[8] S. Srinivas, C.V. Joga Rao, A.K. Rao, An exact analysis for vibration of simply-supported homogeneous and laminated thick rectangular plates, *Journal of Sound and Vibration* 12 (1970) 187–199.

[9] M. Levinson, Free vibrations of a simply supported, rectangular plates: an exact elasticity solution, *Journal of Sound and Vibration* 98 (1985) 289–298.

[10] W.H. Wittrick, Analytical three-dimensional elasticity solutions to some plate problems, and some observations on Mindlin's plate theory, *International Journal of Solids and Structures* 23 (1987) 441–464.

[11] R.C. Batra, S. Aimmanee, Missing frequencies in previous exact solutions of free vibrations of simply supported rectangular plates, *Journal of Sound and Vibration* 265 (2003) 887–896.

[12] K.T. Sundara Raja Iyengar, P.V. Raman, Free vibration of rectangular plates of arbitrary thickness, *Journal of Sound and Vibration* 54 (1977) 229–236.

[13] K.T. Sundara Raja Iyengar, P.V. Raman, Free vibration of rectangular plates of arbitrary thickness with one or more edges clamped, *Journal of Sound and Vibration* 71 (1980) 463–472.

[14] M. Malik, C.W. Bert, Three-dimensional elasticity solutions for free vibrations of rectangular plates by the differential quadrature method, *International Journal of Solids and Structures* 35 (1998) 299–318.

[15] K.M. Liew, T.M. Teo, Three-dimensional vibration analysis of rectangular plates based on differential quadrature method, *Journal of Sound and Vibration* 220 (1999) 577–599.

[16] K.M. Liew, T.M. Teo, J.B. Han, Comparative accuracy of DQ and HDQ methods for three-dimensional vibration analysis of rectangular plates, *International Journal for Numerical Methods in Engineering* 45 (1999) 1831–1848.

[17] C.P. Filipich, M.B. Rosales, P.N. Bellés, Natural vibration of rectangular plates considered as tridimensional solid, *Journal of Sound and Vibration* 212 (1998) 599–610.

[18] J.R. Hutchinson, S.D. Zillimer, Vibration of a free rectangular parallelepiped, *ASME Journal of Applied Mechanics* 50 (1983) 123–130.

[19] A. Fromme, A.W. Leissa, Free vibration of the rectangular parallelepiped, *Journal of Acoustical Society of America* 48 (1970) 290–298.

[20] K.K. Ten, K.C. Brown, On the three-dimensional analysis of thick laminated plates, *Journal of Sound and Vibration* 88 (1983) 213–224.

[21] T. Mizusawa, S. Takagi, Application of the spline prism method to analyze vibration of thick rectangular plates with two opposite edges simply supported, *Communications in Numerical Methods in Engineering* 11 (1995) 1–11.

[22] Y.K. Cheung, S. Chakrabarti, Free vibration of thick, layered rectangular plates by a finite layer method, *Journal of Sound and Vibration* 21 (1972) 277–284.

[23] D. Zhou, Y.K. Cheung, J. Kong, Free vibration of thick, layered rectangular plates with point supports by finite layer method, *International Journal of Solids and Structures* 37 (2000) 1483–1499.

[24] A. Houmat, Three-dimensional free vibration analysis of plates using the *h-p* version of the finite element method, *Journal of Sound and Vibration* 290 (2006) 690–704.

[25] A.W. Leissa, Z. Zhang, On the three-dimensional vibrations of cantilevered rectangular parallelepiped, *Journal of the Acoustical Society of America* 73 (1983) 2013–2021.

[26] O.G. McGee, A.W. Leissa, Three-dimensional free vibrations of thick skewed cantilevered plate, *Journal of Sound and Vibration* 144 (1991) 305–322.

[27] K. Itakura, Free vibration analysis of thick skewed plates having arbitrary boundary conditions, *AIJ Journal of Structural and Construction Engineering* 492 (1997) 37–45 (in Japanese).

[28] W.C. Lim, Three-dimensional vibration analysis of a cantilevered parallelepiped: Exact and approximate solutions, *Journal of the Acoustical Society of America* 106 (1999) 3375–3381.

[29] K. Suda, K. Itakura, M. Okuno, Three-dimensional free vibration analysis of cantilevered thick plates with skewed fixed end, *AIJ Journal of Structural and Construction Engineering* 519 (1999) 35–39 (in Japanese).

[30] K.M. Liew, K.C. Hung, K.M. Lim, A continuum three-dimensional vibration analysis of thick rectangular plates, *International Journal of Solids and Structures* 30 (1993) 3357–3379.

[31] K.M. Liew, K.C. Hung, K.M. Lim, Three-dimensional vibration of rectangular plates: variance of simple support conditions and influence of in-plane inertia, *International Journal of Solids and Structures* 31 (1994) 3233–3247.

[32] K.M. Liew, K.C. Hung, K.M. Lim, Free vibration studies on stress-free three-dimensional elastic solid, *ASEM Journal of Applied Mechanics* 62 (1995) 159–165.

[33] K.M. Liew, K.C. Hung, K.M. Lim, Three-dimensional vibration of rectangular plates: effects of thickness and edge constraints, *Journal of Sound and Vibration* 182 (1995) 709–727.

[34] D. Zhou, Y.K. Cheung, F.T.K. Au, S.H. Lo, Three-dimensional vibration analysis of thick rectangular plates using Chebyshev polynomial and Ritz method, *International Journal of Solids and Structures* 39 (2002) 6339–6353.

[35] D. Zhou, Y.K. Cheung, S.H. Lo, F.T.K. Au, Three-dimensional vibration analysis of rectangular plates with mixed boundary conditions, *ASEM Journal of Applied Mechanics* 72 (2005) 227–236.

[36] I.J. Schoenberg, Contributions to the problem of approximation of equidistant data by analytic functions, *Quarterly of Applied Mathematics* 4 (1946) 45–99, 112–141.

[37] H.B. Curry, I.J. Schoenberg, On the spline distributions and their limits, the polya distributions, *Bulletin of the American Mathematical Society* 53 (1947) 1114.

[38] H.B. Curry, I.J. Schoenberg, On polya frequency functions IV: the fundamental spline functions and their limits, *Journal d'Analyse Mathématique* 17 (1966) 71–107.

[39] C.D. Boor, On calculating with B-splines, *Journal of Approximation Theory* 6 (1972) 50–62.

[40] R. Kao, On the treatment of boundary conditions by the method of artificial parameters, *International Journal for Numerical Methods in Engineering* 8 (1974) 425–429.

[41] Y. Xiang, C.M. Wang, S. Kitipornchai, Exact vibration solution for initially stressed Mindlin plates on Pasternak foundations, *International Journal of Mechanical Science* 36 (1994) 311–316.

[42] K.M. Liew, Y. Xiang, S. Kitipornchai, Transverse vibration of thick rectangular plates-I. Comprehensive sets of boundary conditions,, *Computers and Structures* 49 (1993) 1–29.

[43] A.W. Leissa, The vibration of rectangular plates, *Journal of Sound and Vibration* 31 (1973) 257–293.

[44] C. Shu, W. Chen, On optimal selection of interior points for applying discretized boundary conditions in DQ vibration analysis of beams and plates, *Journal of Sound and Vibration* 222 (1999) 239–257.

[45] T. Mikami, J. Yoshimura, Application of the collocation method to vibration analysis of rectangular Mindlin plates, *Computers and Structures* 18 (1984) 425–431.

[46] C.W. Lim, K.M. Liew, S. Kitipornchai, Numerical aspects for free vibration of thick plates. Part I: Formulation and verification, *Computer Methods in Applied Mechanics and Engineering* 156 (1998) 15–29.